

周伏顺,林鑫,王郅睿,等. 闽北邵武地区玄武安山岩的成因和意义:来自年代学、地球化学及 Nd-Hf 同位素的约束. 吉林大学学报(地球科学版), 2024, 54(3): 840-861. doi:10.13278/j.cnki.jjuese.20230345.

Zhou Fushun, Lin Xin, Wang Zhirui, et al. Petrogenesis and Significance of Basaltic Andesite in the Shaowu Area, Northern Fujian: Constraints from Geochronology, Geochemistry and Nd-Hf Isotopes. Journal of Jilin University (Earth Science Edition), 2024, 54(3): 840-861. doi:10.13278/j.cnki.jjuese.20230345.

闽北邵武地区玄武安山岩的成因和意义

——来自年代学、地球化学及 Nd-Hf 同位素的约束

周伏顺, 林鑫, 王郅睿, 邵程波

长安大学地球科学与资源学院, 西安 710054

摘要: 东南沿海地区中生代火山岩研究成果颇丰, 但有关中侏罗世晚期基性火山岩的报道较少, 限制了对该区域中生代构造-岩浆活动及大地构造演化的深入理解。本文对江绍断裂带东南侧邵武地区的中生代火山岩开展了系统的岩石学、锆石 U-Pb 年代学、锆石 Lu-Hf 同位素、地球化学和 Sm-Nd 同位素研究。结果显示: 邵武地区玄武安山岩喷发年龄为 (161.0 ± 2.0) Ma; 同位素地球化学结果显示, 这些样品中一晚侏罗世锆石的 $\epsilon_{\text{Hf}}(t)$ 值介于 $-14.33 \sim -10.41$ 之间, $\epsilon_{\text{Nd}}(t)$ 值较低 ($-9.2 \sim -8.4$), 反映富集 Nd 同位素的特征; 岩石地球化学结果表明, 该套火山岩具有高 $w(\text{Al}_2\text{O}_3)$ 、 $w(\text{Na}_2\text{O})$ 、低 $w(\text{MgO})$ 、 $w(\text{TFe}_2\text{O}_3)$ 等特征, 稀土总量较低, 稀土配分曲线为右倾型, 且具弱的 Eu 负异常, 大离子亲石元素 Rb、Ba 和 K 相对富集, 高场强元素 Nb、Ta、Ti、P 等相对亏损。综合岩石学和地球化学研究结果, 本文认为邵武玄武安山岩起源于交代岩石圈地幔的部分熔融, 并经历一定结晶的分异作用, 其大地构造背景总体为板内环境。结合前人对区域构造-岩浆活动的认识, 本文认为在中侏罗世晚期, 太平洋俯冲板片发生回撤、撕裂, 导致幔源岩浆底侵并置换了古老壳源岩石, 从而东南沿海地区虽整体处于挤压背景, 但仍存在局部拉张环境。

关键词: 中侏罗世; 地球化学; 伸展背景; 玄武安山岩; 东南沿海

doi: 10.13278/j.cnki.jjuese.20230345

中图分类号: P588.145

文献标志码: A

Petrogenesis and Significance of Basaltic Andesite in the Shaowu Area, Northern Fujian: Constraints from Geochronology, Geochemistry and Nd-Hf Isotopes

Zhou Fushun, Lin Xin, Wang Zhirui, Shao Chengbo

School of Earth Sciences and Resources, Chang'an University, Xi'an 710054, China

Abstract: Among the Mesozoic volcanic rocks along the southeast coast of China, Middle Jurassic

收稿日期: 2023-12-21

作者简介: 周伏顺(1997—), 男, 硕士研究生, 主要从事地球化学方面的研究, E-mail: z913909811@163.com

通信作者: 林鑫(1987—), 男, 副教授, 主要从事应用地球化学及其与数据科学交叉领域方面的研究, E-mail: xinlin@chd.edu.cn

基金项目: 陕西省重点研发计划(2024GH-ZDXM-26); 国家重点研发计划(2016YFC0600601); 中央高校基金项目(300102271206)

Supported by the Key Research and Development Program of Shaanxi (2024GH-ZDXM-26), the National Key Research and Development Program(2016YFC0600601) and the Central University Fund Project (300102271206)

rocks are seldom reported, yet they hold significant importance for understanding Mesozoic magmatic activities and tectonic evolution in this region. The Shaowu basaltic andesite, exposed in the southeast of the Jiangshao fault zone, provides an ideal opportunity for study. This paper systematically presents petrological, zircon U-Pb geochronological, Lu-Hf isotopic, whole-rock geochemistry and Sm-Nd isotopic analyses of the basaltic andesite, indicating an eruption age of (161.0 ± 2.0) Ma. The isotopic data shows that all samples are characterized by $\epsilon_{\text{Hf}}(t)$ values ranging from -14.33 to -10.41 and low $\epsilon_{\text{Nd}}(t)$ values between -9.2 to -8.4 . The geochemical results shows high $w(\text{Al}_2\text{O}_3)$ and $w(\text{Na}_2\text{O})$ contents, along with low levels of $w(\text{MgO})$ and $w(\text{TFe}_2\text{O}_3)$ etc. The total rare earth elements (REE) content is low, with chondrite-normalized REE patterns showing LREE enrichment and weak Eu negative anomalies. Furthermore, large ion lithophile elements such as Rb, Ba and K are enriched, while the high field strength elements such as Nb, Ta, Ti and P are relatively depleted. The geochemical and petrological characteristics of the basaltic andesite imply that it originated from partial melting of a metasomatic mantle wedge, underwent certain crystallization differentiation, and formed in an intraplate tectonic environment. Based on previous studies on regional tectonic-magmatic activities, it is proposed that Pacific subducted plate retreat and tearing, resulting in encroachment of mantle-derived magma and the replacement of ancient crust-derived rocks, occurred amidst local extension within the broader compressional background of the south-eastern coast of China during the Middle Jurassic.

Key words: Middle Jurassic; geochemical; extensional setting; basaltic andesite; southeast coast of China

0 引言

玄武安山岩直接导源于上地幔,受地幔源岩成分的制约,其岩浆的形成与全球构造,如裂谷扩张、板块俯冲消减及地幔的深部作用(地幔对流、局部隆升、流体交代)等过程有关。因此,玄武安山岩研究对于反演地幔物质成分、分析构造环境及地球深部动力学均具重大意义^[1],是国际火山岩研究的热点^[2-5]。

华南地区以大面积分布的岩浆岩^[6]及金属矿床^[7]为特色,其内部可划分出多个构造带^[8]及成矿带^[9],使得该地区成为国内外学者研究的热点地区之一。现有研究表明,这些大规模的岩浆及矿床多与晚中生代的火山作用密切相关,并被普遍解释为是古太平洋板块向欧亚大陆俯冲作用所造成的应力体制转换的产物。然而,前人^[10-11]对于转换的时限是否为中侏罗世目前还存在争议。目前,对于该时期华南地区的应力状态也相应存在不同的观点,主要包括:由挤压转为伸展体制^[10]、挤压体制^[11]以及整体挤压体制下的局部伸展^[6]。

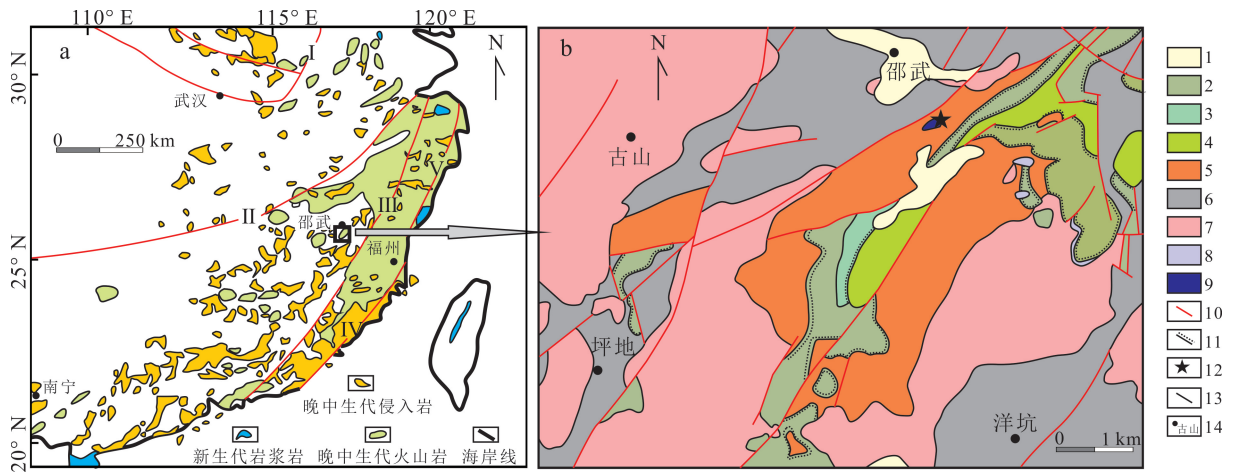
玄武安山岩作为深部地质过程的记录者,能够为理解造山带构造演化过程提供很好的窗口,也为解决上述争议提供了新的思路。闽北地区侏罗纪火山岩广泛发育,其成因及构造背景的界定对于确定区域构

造格架及演化起着至关重要的作用。该地区火山岩以大规模中酸性火山岩为主^[12-17],而对于玄武安山岩的报道较少。本文以邵武地区采集的玄武安山岩为研究对象,通过对样品进行岩石学、年代学、锆石 Lu-Hf 同位素、全岩地球化学以及 Sm-Nd 同位素的研究,确定玄武安山岩的形成时代及其成因,阐明中侏罗世古太平洋板块俯冲作用对闽北地区的影响。

1 地质背景及样品描述

华南板块由扬子地块、华夏地块以及其间的缝合带—江南造山带共同组成^[18-21],南北方向上分别夹持于东南亚块体和秦岭造山带之间,西邻青藏高原,东侧为太平洋板块。自元古宙板块拼合以来,华南板块经历了多阶段的构造-岩浆活动,成为研究大陆体制转换的理想区域^[22-23]。其中,中生代板块间构造体制的变化导致了区域巨量岩浆的侵位(图 1a),引发了华南大规模的成矿事件,成为国内外地质学家研究的焦点。

扬子地块内部可划分为同一盖层的不同基底,新元古代以来拼合成为稳定的克拉通^[25];华夏地块主要由大面积的新元古代碎屑岩夹火山岩、岩浆岩及碳酸盐岩组成。新元古代末期,扬子和华夏地块发生碰撞拼合,形成江南造山带,沿该造山带南界的江绍断裂带分布了大量冷侵位的蛇绿岩套、蓝片岩



I. 郟庐断裂带; II. 江绍断裂带; III. 政和一大埔断裂带; IV. 长乐—南澳断裂带; V. 温州—镇海断裂带。1. 第四系; 2. 侏罗系梨山群; 3. 侏罗系漳平群; 4. 侏罗系兜岭群; 5. 下古生界罗峰溪群; 6. 震旦系; 7. 酸性岩; 8. 安山玢岩; 9. 玄武安山岩; 10. 断层; 11. 角度不整合; 12. 采样位置; 13. 地质界线; 14. 地名。据文献[24]修编。

图1 华南地区岩浆岩分布(a)及研究区地质图(b)

Fig.1 Distribution of igneous rock in South China (a) and geological map of the study area (b)

和具岛弧属性的岩浆岩^[26-27]。加里东期和印支期华南板块经历了两期陆内造山运动,主要体现在扬子地块东半部和整个华夏地块,区域内岩石卷入强烈变质变形过程中^[25]。尤其是加里东期造山运动使得前泥盆纪岩石大多变质成为片岩、片麻岩和混合岩,且伴随强烈的岩浆活动,形成变质变形岩石—花岗岩复合体系^[27]。

邵武地区位于华夏地块中北部,区域出露的地层由老到新依次为:震旦系、下古生界罗峰溪群、侏罗系(图1b)。震旦系为黑云母斜长片麻岩、云母片岩夹斜长角闪岩,变质程度达角闪岩相,且发育强烈的混合岩化作用^[28-29]。下古生界罗峰溪群为灰绿色变砂岩、千枚岩、片岩,局部夹大理岩。侏罗系通过断层与下古生界分隔,内部岩石单元包括:兜岭群,下部为砂岩夹凝灰岩及灰岩透镜体,上部为晶屑凝灰岩;漳平群,为红绿相间的粉砂岩及细砂岩;梨山群,分为下部的灰黑色砂砾岩、粗砂岩、粉砂岩及上部的砂岩夹灰岩透镜体。研究区南东侧及北西侧分别出露NE走向的政和一大埔断裂带及江绍断裂带,区内断裂构造发育,包括NE向、NW向及EW向等多组,其中近NE向最为发育。区内岩浆岩主要为印支期和燕山期黑云母花岗岩,侵入于震旦系中,其次是玄武安山岩和闪长岩,零星分布于下古生界罗峰溪群中^[30]。

本次研究的玄武安山岩出露于邵武市南侧的罗峰溪群千枚岩中,规模较小,呈NE向延伸,长度约

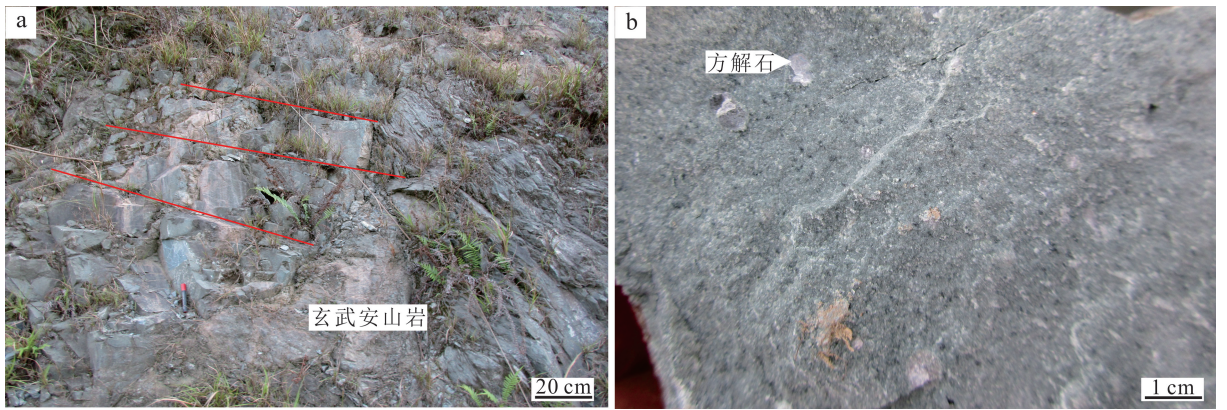
300 m,宽度约100 m。由于植被覆盖,玄武安山岩与千枚岩接触界面不易观察,岩石表面风化较强,呈黄褐色,而人工揭露的断面上岩石相对新鲜,呈深灰色,节理发育(图2a),十分破碎。岩石表面可见气孔构造,内部被方解石矿物充填(图2b)。

镜下观察显示,玄武安山岩具间粒-间隐结构,块状构造,斑晶体积分数为35%~40%,多为斜长石,自形板状,表面可见弱绢云母化,粒径为0.2~0.5 mm,见少量石英,粒径多为0.1~0.2 mm。局部可见杏仁体,主要由方解石和石英充填,大小为1.0~1.5 mm,体积分数为5%~10%。基质由细粒斜长石和辉石等组成,基质中见半自形粒状的次生绿帘石和次生方解石(图3)。根据岩石结构、构造及矿物成分组成,定名为玄武质安山岩。

2 分析方法

本次工作采集了露头上较新鲜的玄武安山岩样品,采样位置见图1b。选择其中1件样品进行年代学及锆石Lu-Hf同位素分析,4件样品进行全岩主微量及稀土元素、Sm-Nd同位素测试。

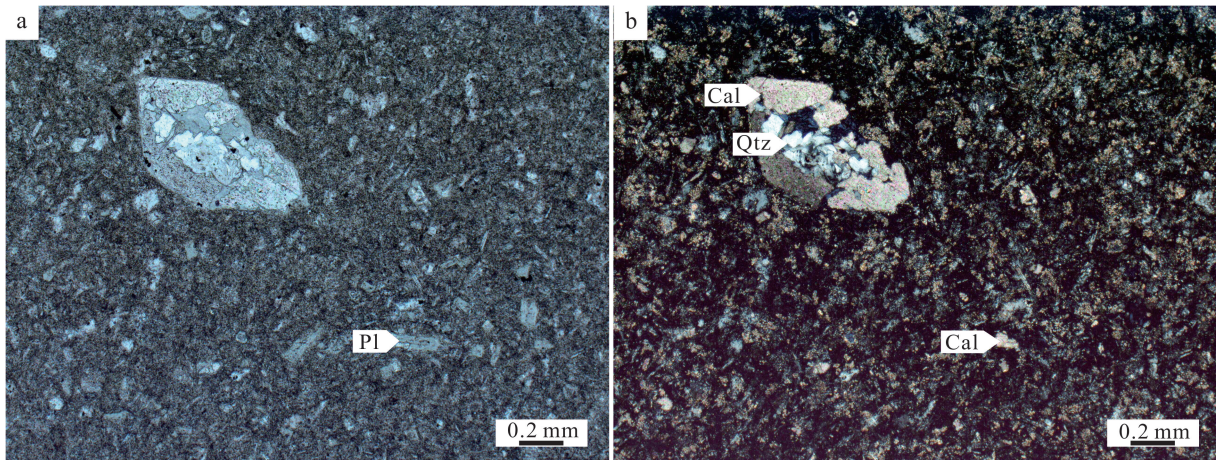
锆石单矿物挑选在河北省廊坊市尚艺岩矿检测技术有限公司完成。将野外采集的样品粉碎,通过常规重选法选出单矿物,在双目镜下挑选出形态较好的锆石。锆石制靶在南京宏创地质勘查技术服务有限公司完成。首先通过环氧树脂将待测锆石和标准锆石固定在玻璃板上,然后抛光至锆石暴露出



a. 玄武安山岩节理;b. 玄武安山岩内部杏仁体。

图2 邵武地区玄武安山岩野外和手标本特征

Fig.2 Outcrops and samples of the basaltic andesite in the Shaowu area



Qtz. 石英; Cal. 方解石; Pl. 斜长石。

图3 邵武地区玄武安山岩显微特征照片

Fig.3 Micrographs of the basaltic andesite in the Shaowu area

中心面,在偏光显微镜下对锆石进行反射光和透射光拍照,确定锆石的包体以及裂纹情况,最后进行阴极发光(CL)照相,以检查锆石的内部结构。

选择晶形较好,无包体、裂纹的锆石颗粒进行锆石U-Pb测年分析。锆石分析在中国地质科学院矿产资源研究所使用电感耦合等离子体质谱仪(LA-MC-ICP-MS)完成,详细的仪器参数和分析流程见文献[31]。仪器的型号和相应的激光剥蚀系统分别为 Finnigan Neptune 型 LA-MC-ICP-MS 和 NewWave UP213 nm。实验过程采用单点剥蚀,直径为 30 μm ,采样深度为 20~40 μm ,频率为 10 Hz,输出能量约为 2.5 J/cm^2 。实验过程采用 He 作为载气。锆石年龄以 GJ-1 为外标,元素质量分数以 M217 为外标。在测试过程中,每隔 10 个

样品点测试 2 个 GJ-1 和 1 个 Plesovice 标准锆石。最后使用 ICPMSDataCal 软件完成数据处理(信号选择、漂移校正和年龄计算),通过 Isoplot3.0 软件计算加权平均年龄。

锆石 Lu-Hf 同位素测定在北京科荟测试技术有限公司完成,仪器为激光剥蚀多接收器电感耦合等离子体质谱仪(Neptune plus),激光进样系统为 RESOLUTION SE 固体激光器。根据锆石照片选择合适区域,利用激光剥蚀系统对锆石进行剥蚀。测点位置为 U-Pb 年龄的同一测点或其附近。激光剥蚀的斑束直径为 30~38 μm ,能量密度为 6 J/cm^2 ,频率为 6 Hz,激光剥蚀物质以高纯 He 为载气送入 Neptune Plus(MC-ICP-MS),积分时间为 27 s。锆石样品 GJ-1 用作分析的参考标准。在分析过程中,

GJ-1 标准的 $^{176}\text{Hf}/^{177}\text{Hf}$ 加权平均值为 $0.282\ 007 \pm 0.000\ 007(2\sigma, n=36)$, 与误差范围内的报告值一致。采用 $^{179}\text{Hf}/^{177}\text{Hf} = 0.7325$ 对 Hf 同位素比值进行指数归一化质量歧视校正, 采用 $^{173}\text{Yb}/^{172}\text{Yb} = 1.35274$ 对 Yb 同位素比值进行指数归一化质量歧视校正。由于锆石中 $^{176}\text{Lu}/^{177}\text{Hf}$ 值通常小于 0.002, 因此锆石中 ^{176}Hf 的同质异位素的干扰主要来自 ^{176}Yb 。在锆石激光剥蚀过程中直接测定 Yb 信号, 用剥蚀过程中 β_{Yb} 的平均值作为 Yb 的质量歧视校正系数来进行同质异位素 ^{176}Yb 的干扰校正。

岩石样品主、微量及稀土元素测定在北京燕都中实测试技术有限公司完成。将岩石粗碎至厘米级的碎块, 选取无蚀变及脉体穿插的新鲜样品用纯化水冲洗干净, 烘干并粉碎至 200 目备用。主量元素测试: 首先将粉末样品称量后加入 $\text{Li}_2\text{B}_4\text{O}_7(1:8)$ 助熔剂混合, 然后使用融样机加热至 $1\ 150\ ^\circ\text{C}$ 使其在金铂坩埚中熔融成均一玻璃片体, 最后使用 XRF (Zetium, PANalytical) 测试, 测试结果保证数据误差小于 1%。微量及稀土元素测试: 首先将 200 目粉末样品称量并置放入聚四氟乙烯溶样罐并加入 $\text{HF} + \text{HNO}_3$, 然后在干燥箱中将高压消解罐保持在 $190\ ^\circ\text{C}$ 温度 72 h, 最后取出经过赶酸并将溶液定容为稀溶液上机测试。测试使用 ICP-MS (M90, analytikjena) 完成, 所测数据根据监控标样 GSR-2 显示误差小于 5%, 部分挥发性元素及极低质量分数元素的分析误差小于 10%。

Sm-Nd 同位素测定在核工业北京地质研究院

使用 ISOPROBE-T 热电离质谱仪进行。详细的化学制备、质谱法和标准样品测定见文献[32]。使用 $^{143}\text{Nd}/^{144}\text{Nd} = 0.7219$ 校正 Nd 同位素分析质量, 测定过程中标准样品的测量结果如下: 基准物质 $\text{JMC} = 0.521109 \pm 3.000000(^{143}\text{Nd}/^{144}\text{Nd})$ 。Sm 和 Nd 的分析空白总量为 $5 \times 10^{-11}\ \text{g}$ 。

3 分析结果

3.1 锆石年龄

玄武安山岩中的锆石大多为短柱状, 粒径 $50 \sim 150\ \mu\text{m}$, 长宽比为 $1:1 \sim 1.5:1$ 。在 CL 图像中可见其具有清晰的振荡环带(图 4), 具有岩浆锆石的特征。选取 29 颗发育环带的锆石进行 U-Pb 同位素测试分析, 测试结果见表 1。结果显示所有分析点的 Th/U 值均大于 0.1, 这也反映其锆石为岩浆成因。其中一个测点的 $^{206}\text{Pb}/^{238}\text{U}$ 年龄为 234.4 Ma, 结合其 CL 测点位置认为该数值代表了样品中锆石的混合年龄。其余锆石分析年龄可以分为两组, 在锆石年龄谐和图上, 7 个年龄数据点的 $^{206}\text{Pb}/^{238}\text{U}$ 年龄为 $458.0 \sim 443.2\ \text{Ma}$, 其加权平均年龄为 $(449.6 \pm 5.3)\ \text{Ma}$ ($n=7$, $\text{MSWD}=0.49$) (图 4a); 其余 21 个数据点 $^{206}\text{Pb}/^{238}\text{U}$ 年龄为 $168.1 \sim 151.4\ \text{Ma}$, 其加权平均年龄为 $(161.0 \pm 2.0)\ \text{Ma}$ ($n=21$, $\text{MSWD}=2.5$) (图 4b)。

3.2 锆石 Lu-Hf 同位素

玄武安山岩中锆石 Lu-Hf 同位素分析结果见图 5 及表 2。样品 FJ11-5 中的 12 颗锆石加权平均

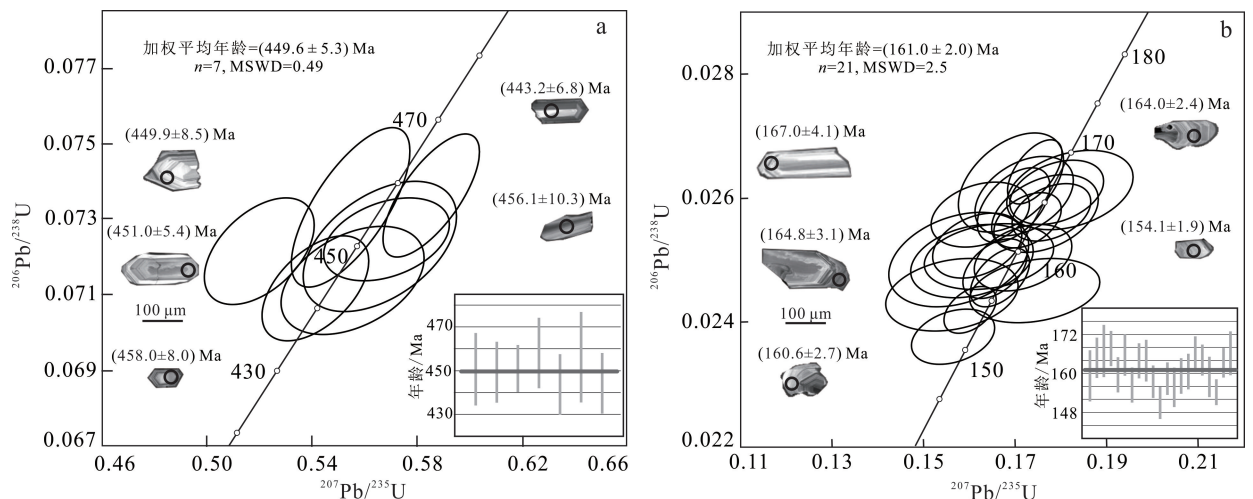


图 4 邵武地区玄武安山岩锆石 CL 图像、测点位置及年龄谐和图

Fig. 4 Representative zircon cathodoluminescence images, analysed spots and concordia diagrams of the basaltic andesite in the Shaowu area

表 1 邵武地区玄武安山岩锆石的 U-Th-Pb 同位素分析结果
Table 1 U-Th-Pb isotopic analyses for zircon from the basaltic andesite in the Shaowu area

点号	$^{238}\text{Th}/^{232}\text{Th}$		Th/U	同位素比值				年龄/Ma							
	^{238}U	^{238}U		$^{207}\text{Pb}/^{206}\text{Pb}$	$^{207}\text{Pb}/^{235}\text{U}$	$^{206}\text{Pb}/^{238}\text{U}$	$^{207}\text{Pb}/^{206}\text{Pb}$	$^{207}\text{Pb}/^{235}\text{U}$	$^{206}\text{Pb}/^{238}\text{U}$	$^{206}\text{Pb}/^{238}\text{U}$	$^{206}\text{Pb}/^{238}\text{U}$				
1	96	95	1.01	0.057 1	0.002 3	0.565 7	0.023 8	0.072 3	0.001 4	494.5	61.1	455.3	15.4	449.9	8.5
2	124	121	1.02	0.052 4	0.001 6	0.520 0	0.017 0	0.072 2	0.001 2	301.9	68.5	425.2	11.4	449.2	6.9
3	188	72	2.60	0.047 2	0.004 1	0.157 7	0.012 4	0.025 0	0.000 6	57.5	192.6	148.7	10.9	159.2	3.9
4	138	157	0.88	0.057 4	0.002 1	0.568 3	0.019 5	0.072 5	0.000 9	509.3	76.8	456.9	12.6	451.0	5.4
5	550	361	1.52	0.047 5	0.001 5	0.169 7	0.006 4	0.025 9	0.000 5	76.0	74.1	159.1	5.6	164.8	3.1
6	578	132	4.38	0.046 9	0.002 4	0.169 1	0.009 4	0.026 2	0.000 7	55.7	109.3	158.6	8.1	167.0	4.1
7	754	622	1.21	0.048 1	0.001 2	0.174 3	0.004 8	0.026 4	0.000 4	101.9	61.1	163.1	4.2	168.1	2.7
8	431	309	1.40	0.057 5	0.001 1	0.585 3	0.015 0	0.073 6	0.001 3	522.3	38.0	467.9	9.6	458.0	8.0
9	176	87	2.03	0.048 2	0.003 7	0.164 3	0.011 6	0.025 1	0.000 4	109.4	170.3	154.5	10.1	159.5	2.7
10	626	348	1.80	0.048 4	0.002 3	0.172 0	0.008 8	0.026 0	0.000 5	120.5	86.1	161.2	7.6	165.7	3.3
11	400	257	1.55	0.050 5	0.002 9	0.174 3	0.011 6	0.024 5	0.000 4	220.4	133.3	163.1	10.0	156.1	2.7
12	202	124	1.63	0.046 7	0.002 8	0.162 4	0.008 8	0.025 7	0.000 4	31.6	137.0	152.8	7.7	163.8	2.7
13	234	145	1.61	0.050 7	0.002 7	0.176 5	0.009 5	0.025 8	0.000 5	227.8	120.4	165.1	8.2	163.9	3.2
14	299	188	1.59	0.051 1	0.001 9	0.259 9	0.009 7	0.037 0	0.000 6	242.7	78.7	234.6	7.8	234.4	3.4
15	392	289	1.35	0.049 4	0.001 6	0.166 7	0.005 3	0.024 7	0.000 4	164.9	75.9	156.6	4.6	157.4	2.5
16	374	221	1.69	0.047 9	0.002 3	0.156 4	0.007 4	0.023 8	0.000 4	94.5	116.7	147.5	6.5	151.4	2.3
17	1 364	340	4.01	0.048 6	0.001 7	0.165 6	0.005 7	0.024 9	0.000 4	131.6	76.8	155.6	5.0	158.3	2.5
18	180	77	2.34	0.046 2	0.003 5	0.156 3	0.011 8	0.024 4	0.000 5	9.4	179.6	147.4	10.4	155.7	3.0
19	243	148	1.64	0.050 0	0.002 4	0.171 8	0.008 7	0.025 0	0.000 4	194.5	112.9	161.0	7.5	159.4	2.8
20	359	218	1.65	0.046 9	0.002 3	0.161 7	0.008 0	0.025 2	0.000 4	55.7	105.5	152.2	7.0	160.6	2.7
21	122	125	0.98	0.056 0	0.001 8	0.541 3	0.016 6	0.071 2	0.001 1	453.8	67.6	439.3	10.9	443.2	6.8
22	263	186	1.42	0.049 7	0.002 3	0.179 1	0.008 3	0.026 1	0.000 4	189.0	104.6	167.3	7.2	166.1	2.7
23	369	245	1.51	0.050 6	0.002 1	0.178 0	0.007 0	0.025 8	0.000 4	233.4	99.1	166.3	6.1	164.0	2.4
24	346	83	4.16	0.047 7	0.003 4	0.160 5	0.010 9	0.025 0	0.000 5	83.4	159.2	151.2	9.6	159.0	3.0
25	588	402	1.46	0.048 2	0.001 4	0.160 2	0.004 7	0.024 2	0.000 3	109.4	75.0	150.8	4.1	154.1	1.9
26	431	256	1.68	0.054 8	0.001 3	0.554 6	0.018 4	0.073 3	0.001 7	466.7	51.8	448.0	12.0	456.1	10.3
27	516	397	1.30	0.048 9	0.001 6	0.172 7	0.006 0	0.025 6	0.000 4	142.7	79.6	161.8	5.2	163.2	2.3
28	114	99	1.15	0.056 9	0.002 3	0.555 5	0.022 1	0.071 4	0.001 2	500.0	90.7	448.6	14.5	444.5	7.1
29	297	180	1.65	0.050 9	0.003 0	0.182 0	0.011 3	0.026 1	0.000 5	235.3	134.2	169.8	9.7	166.3	3.3

年龄为 161 Ma, 其 $(^{176}\text{Hf}/^{177}\text{Hf})_i$ 值和 $\epsilon_{\text{Hf}}(t)$ 值分别为 0.282 28~0.282 39 和 -14.33~-10.41, 对应于 Hf 地壳 T_{DMC} 为 2 096~1 847 Ma。4 颗锆石的加权平均年龄为 450 Ma, 其 $(^{176}\text{Hf}/^{177}\text{Hf})_i$ 值为 0.282 22~0.282 25, $\epsilon_{\text{Hf}}(t)$ 值为 -10.08~-8.98, 对应于 2 040~1 977 Ma 的 T_{DMC} 。

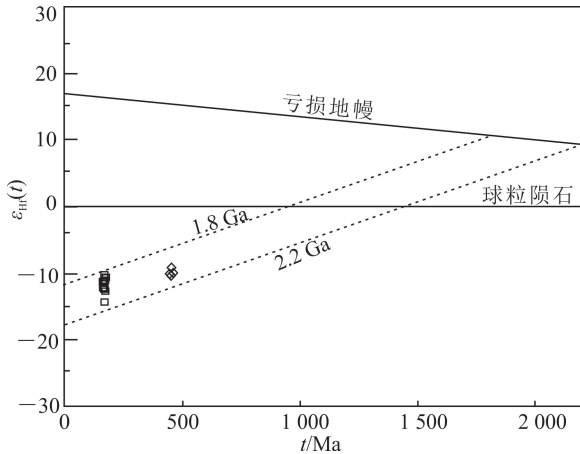


图 5 邵武地区玄武安山岩锆石 $\epsilon_{\text{Hf}}(t)-t$ 图解

Fig. 5 $\epsilon_{\text{Hf}}(t)-t$ plot for the zircons from basaltic andesite in the Shaowu area

3.3 主、微量及稀土元素

玄武安山岩的主量元素分析结果见表 3。由于采集的样品发生了轻微蚀变, 因此在进行元素分析时, 尽量不采用对蚀变作用比较敏感的 Rb、Ba、K、Si 等活性元素, 而利用不活泼的 Ti、Zr、Nb、Y、Ta、Hf 及稀土元素来判别岩石类型^[33-34]。 $\omega(\text{Th})-\omega(\text{Co})$ 和 $\text{Zr} \times 0.0001/\text{TiO}_2 - \text{Nb}/\text{Y}$ 判别图(图 6)^[35-36]中, 采集的样品大多落入安山岩或玄武安山岩的范围, 综合样品岩相学中较高的石英体积分数、长石的宽板状形态以及测年样品中挑选出的锆石形态, 认为样品应属于钙碱性玄武安山岩。

玄武安山岩样品的 SiO_2 质量分数为 50.80%~52.48%, MgO 质量分数为 5.40%~6.59%, TFe_2O_3 质量分数为 8.04%~8.54%, TiO_2 质量分数为 0.92%~1.02%, Al_2O_3 质量分数为 14.50%~15.64%, $\text{Mg}^\#$ 值为 55~59。主量元素分析中产生了较高的烧失量(6.70%~7.36%), 因此, 需要对后期蚀变作用是否对活性元素产生影响进行判别^[37]。活性元素 SiO_2 与相对不活动的元素 Ce 之间明显负相关, 而 K_2O 、Rb、Th 与其明显正相关(图 7), 这些元素在岩石后期蚀变过程中受到的影

响较小, 其质量分数的变化是由岩浆作用产生的。另外, 在稀土元素及微量元素图解(图 8)中, 4 个样品呈现出大致相同的变化规律, 也指出玄武安山岩样品的化学成分没有受到后期蚀变作用的明显改变。

玄武安山岩样品稀土和微量元素质量分数分析结果见表 4。稀土元素总量 $\omega(\Sigma\text{REE})$ 较低, 为 $82.33 \times 10^{-6} \sim 92.40 \times 10^{-6}$ 。在球粒陨石标准化稀土元素配分型式图上(图 8a), 样品总体富集轻稀土, 呈现出轻稀土右倾而重稀土近平坦的样式, 轻重稀土之间分馏较弱 ($\text{LREE}/\text{HREE} = 7.38 \sim 7.71$, $(\text{La}/\text{Yb})_{\text{N}} = 7.69 \sim 8.21$), 表现为弱的负 Eu 异常, δEu 为 0.76~0.84。样品微量元素组成特征见图 8b, 整体富集大离子亲石元素 Rb、Ba 和 K, 相对亏损高场强元素 Nb、Ta、Ti、P。

3.4 Sm-Nd 同位素

玄武安山岩 Sm-Nd 同位素组成相对均匀(表 5), $^{147}\text{Sm}/^{144}\text{Nd}$ 为 0.131 3~0.135 0, $^{143}\text{Nd}/^{144}\text{Nd}$ 为 0.512 104~0.512 139, 低于原始地幔现代值 0.512 638^[39]。采用样品的形成年龄(161 Ma)进行计算, 样品的 $\epsilon_{\text{Nd}}(t) = -9.2 \sim -8.4$, 这些特征表明在岩石形成过程中有大量地壳物质加入。在计算岩石 Nd 模式年龄时, Sm-Nd 同位素的分馏效应会产生明显的影响, 以致其模式年龄结果不合理, 为了减少此类影响, 本文采用两阶段模式计算岩石 Nd 同位素模式年龄, 用以近似代表样品源岩的地壳存留年龄。Nd 单阶段模式年龄(T_{DM})为 2 020~1 890 Ma, 与锆石中 Hf 的模式年龄大体一致。Nd 模式年龄值大多分布在古元古代, 这也进一步表明岩浆形成过程中有新元古代地壳物质的参与。

4 讨论

4.1 火山岩时代

1:20 万顺层幅区调报告中未将本次工作中涉及的玄武安山岩圈出, 但在其周边地区零星圈出了多个安山玢岩露头, 它们呈岩脉产于罗峰溪群内, 时代定为燕山早期^[30]。本次地质考察通过野外和镜下特征认为该地区岩石具有明显的杏仁构造, 且 SiO_2 质量分数变化范围为 50.80%~52.48% ($< 53\%$), 该套岩石属于典型的玄武安山岩。本文选取新鲜样品的 LA-ICP-MS 锆石 U-Pb 定年结果表明, 玄武安山岩内部包含了 (449.6 ± 5.3) Ma 和 (161.0 ± 2.0) Ma 两组年龄。但玄武安山岩产于罗峰溪群内部, 表明其喷发时代应该晚于地层, 罗峰溪群内部的化石表明其时代为晚奥陶世(440 Ma)^[40]。

表 2 邵武地区玄武安山岩锆石 Lu - Hf 同位素分析结果
 Table 2 Lu - Hf isotopic analyses for zircon from the basaltic andesite in the Shaowu area

点号	年龄/Ma	¹⁷⁶ Yb/ ¹⁷⁷ Hf	2σ	¹⁷⁶ Lu/ ¹⁷⁷ Hf	2σ	¹⁷⁶ Hf/ ¹⁷⁷ Hf	2σ	(¹⁷⁶ Hf/ ¹⁷⁷ Hf) _i	ε _{Hf} (t)	ε _{Hf} (现在)	T _{DM1} /Ma	T _{DMC} /Ma	f _{Lu/Hf}
FJ11-5-1	450	0.028 125	0.000 438	0.001 017	0.000 017	0.282 236	0.000 035	0.282 23	-9.70	-19.4	1 433	2 021	-0.97
FJ11-5-4	451	0.019 621	0.000 221	0.000 699	0.000 007	0.282 253	0.000 030	0.282 25	-8.98	-18.8	1 398	1 977	-0.98
FJ11-5-5	165	0.020 416	0.000 544	0.000 708	0.000 017	0.282 349	0.000 030	0.282 35	-11.84	-15.4	1 265	1 937	-0.98
FJ11-5-6	167	0.036 533	0.001 227	0.001 205	0.000 044	0.282 388	0.000 028	0.282 38	-10.47	-14.0	1 227	1 852	-0.96
FJ11-5-7	168	0.035 065	0.000 083	0.001 166	0.000 003	0.282 341	0.000 024	0.282 34	-12.10	-15.7	1 292	1 956	-0.97
FJ11-5-9	160	0.016 032	0.000 208	0.000 572	0.000 007	0.282 361	0.000 034	0.282 36	-11.51	-15.0	1 244	1 913	-0.98
FJ11-5-10	166	0.030 767	0.000 490	0.001 055	0.000 015	0.282 390	0.000 034	0.282 39	-10.41	-14.0	1 219	1 847	-0.97
FJ11-5-17	158	0.052 323	0.001 237	0.001 735	0.000 043	0.282 347	0.000 020	0.282 34	-12.16	-15.5	1 303	1 952	-0.95
FJ11-5-19	159	0.018 291	0.000 265	0.000 621	0.000 007	0.282 344	0.000 019	0.282 34	-12.12	-15.6	1 269	1 951	-0.98
FJ11-5-20	161	0.022 038	0.000 290	0.000 741	0.000 008	0.282 342	0.000 018	0.282 34	-12.18	-15.7	1 276	1 956	-0.98
FJ11-5-21	443	0.027 594	0.000 446	0.000 958	0.000 011	0.282 229	0.000 020	0.282 22	-10.08	-19.7	1 441	2 040	-0.97
FJ11-5-23	164	0.019 477	0.000 082	0.000 655	0.000 002	0.282 361	0.000 019	0.282 36	-11.43	-15.0	1 247	1 911	-0.98
FJ11-5-24	159	0.027 290	0.000 440	0.000 907	0.000 016	0.282 342	0.000 022	0.282 34	-12.23	-15.7	1 282	1 958	-0.97
FJ11-5-26	456	0.005 283	0.000 094	0.000 151	0.000 002	0.282 222	0.000 021	0.282 22	-9.80	-19.9	1 421	2 033	-1.00
FJ11-5-27	163	0.033 009	0.000 351	0.001 076	0.000 011	0.282 365	0.000 015	0.282 36	-11.35	-14.9	1 255	1 905	-0.97
FJ11-5-29	166	0.024 174	0.000 985	0.000 799	0.000 026	0.282 278	0.000 020	0.282 28	-14.33	-17.9	1 367	2 096	-0.98

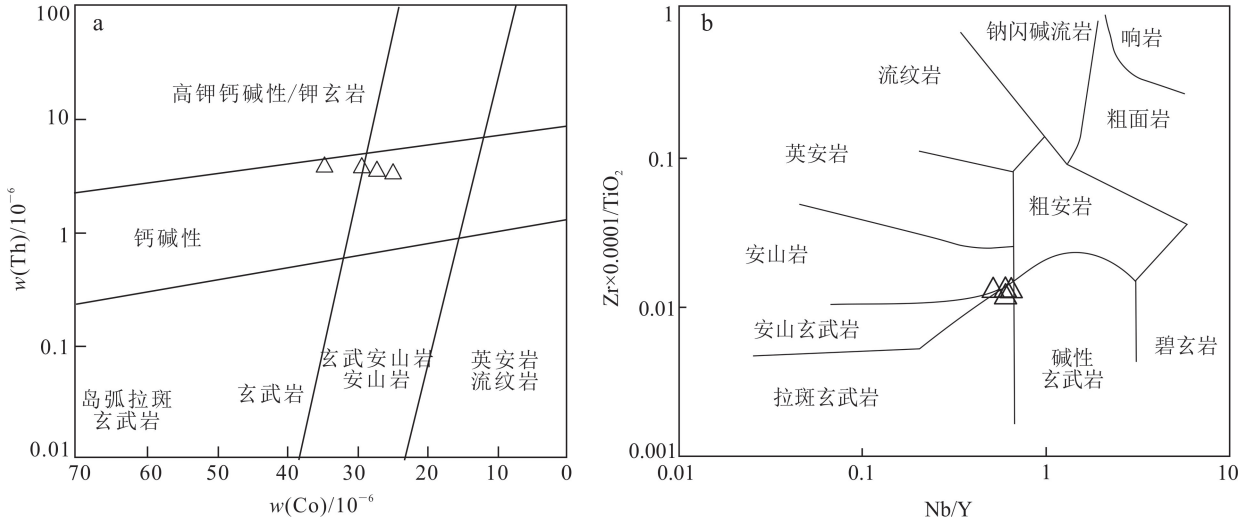
注:ε_{Hf}(现在)为锆石演化至今的ε_{Hf}值;T_{DM1}为一阶段模式年龄;T_{DMC}为二阶段模式年龄;f_{Lu/Hf}为富集系数。

表 3 邵武地区玄武安山岩的主量元素组成分析结果

Table 3 Major element contents of the basaltic andesite in the Shaowu area

样品号	SiO ₂	TiO ₂	Al ₂ O ₃	TFe ₂ O ₃	TFeO	MnO	MgO	CaO	Na ₂ O	K ₂ O	P ₂ O ₅	烧失量	总和	Mg [#]	TFeO/MgO
FJ11-6	52.48	0.96	14.66	8.31	7.48	0.14	5.88	6.49	2.92	1.72	0.18	6.70	100.45	57	1.37
FJ11-7	50.90	1.02	15.64	8.19	7.37	0.12	6.19	5.78	3.15	1.81	0.19	7.00	99.99	58	1.29
FJ11-8	51.13	0.93	14.50	8.04	7.23	0.15	5.40	7.60	2.70	1.76	0.18	7.36	99.76	55	1.46
FJ11-9	50.80	0.92	15.11	8.54	7.68	0.13	6.59	6.32	2.40	2.20	0.17	6.82	100.00	59	1.26

注: Mg[#] 为 MgO 与 (MgO+TFeO) 的分子比; 主量元素质量分数单位为 %。



a. 底图据文献[35]; b. 底图据文献[36]。

图 6 邵武地区玄武安山岩 w(Th)-w(Co) (a) 以及 Zr×0.0001/TiO₂-Nb/Y (b) 图解

Fig.6 w(Th)-w(Co) (a) and Zr×0.0001/TiO₂-Nb/Y (b) plot of the basaltic andesite in the Shaowu area

因此,玄武安山岩中(449.6±5.3) Ma 的年龄不能代表其喷发时代。华南地区在早古生代经历了强烈的构造-热事件,在华夏地块尤为突出,华夏地块的大多数岩石发生变质变形改造及混合岩化,同时也引发了大面积的岩浆活动^[41]。玄武安山岩中(449.6±5.3) Ma 的年龄与华南板块加里东期发育的岩浆事件一致,代表了玄武安山岩形成过程中的岩浆锆石捕虏晶。结合上述讨论,(161.0±2.0) Ma 的年龄应为邵武地区玄武安山岩的喷发时代,为晚侏罗世。

侏罗纪是华南板块重要的构造岩浆活化期,该时期岩浆岩广泛出露,包括中酸性及基性岩浆岩^[42]。其中大量的 A 型花岗岩、双峰火山岩、板内拉斑玄武岩和板内碱性玄武岩分布于南岭构造带^[43]。而东南沿海地区则发育大量的中酸性岩浆岩,如邢光福等^[6]报道了福安地区安山岩的年龄为(162.3±3.7) Ma,张伟等^[13,44]认为浙江松阳毛弄组火山岩的时代为 180~153 Ma。武夷山北缘侏罗纪岩浆活动也有大量的报道和记录,如孟祥金等^[45-46]

认为冷水坑地区的火山岩时代为 160~146 Ma, Wang 等^[47]获得了闽西北地区 I 型花岗岩的时代为 161 Ma。本文年代学结果及上述数据表明,华南东部晚侏罗世大规模岩浆作用形成的火山-侵入岩在闽北邵武地区也有体现,由于晚侏罗世一早白垩世处于华南构造域转换的特殊时期,因此,邵武地区玄武安山岩的厘定对于进一步阐明华南大地构造演化具有很好的指示意义。

4.2 岩石成因

玄武安山岩中相对低 MgO、TFe₂O₃ 质量分数,低 Mg[#] 值(标准地幔的 Mg[#] 值为 68~75^[48]),贫不相容元素 Ni、Co、V,富 Al₂O₃、Na₂O、Sr 等,均显示出演化岩浆的特点。微量元素蛛网图(图 8b)中 Sr、P、Ti 元素的亏损可能与斜长石、磷灰石和 Fe-Ti 氧化物的分离结晶有关。稀土元素配分曲线图(图 8a)中,样品中弱的 Eu 负异常(δEu=0.76~0.84)也暗示了可能存在角闪石或斜长石的分离结晶。w(Sm)-w(Rb)图(图 9a)中可见样品主要分布于含

角闪石的分离结晶趋势线附近。根据 $100(\text{Fe}+\text{Mg}+\text{Mn})/\text{Ti}-100\text{Si}/\text{Ti}$ 图解(图 9b),邵武地区玄武安山岩样品数据分布于单斜辉石分离结晶线附近,同

样说明岩浆演化过程中发生了以单斜辉石为主的分离结晶作用。结合上述特征,笔者认为玄武安山岩岩浆演化过程中发生了一定的结晶分异作用。

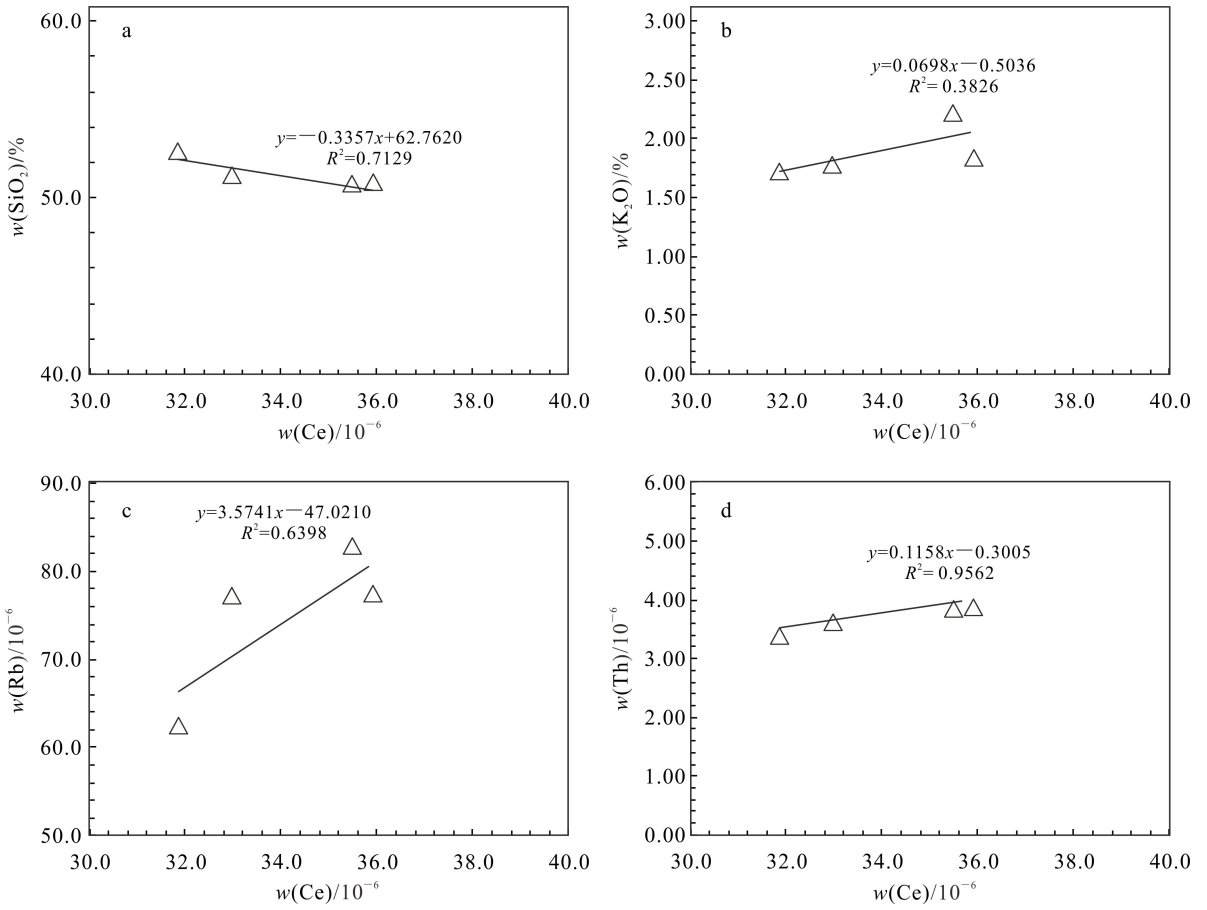
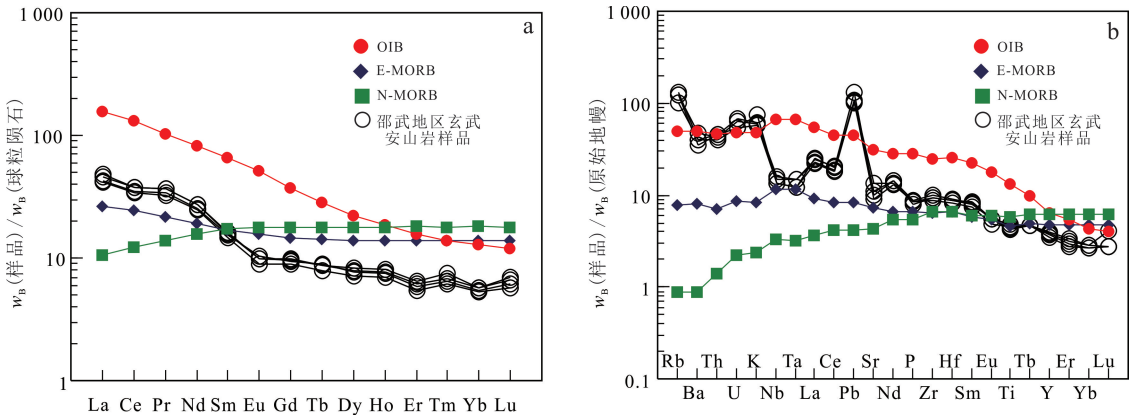


图7 邵武地区玄武安山岩样品 SiO_2 、 K_2O 、Rb 和 Th 对 Ce 相关性图解

Fig.7 Plot of SiO_2 , K_2O , Rb and Th versus Ce contents of the basaltic andesite in the Shaowu area



OIB. 洋岛玄武岩; E-MORB. 富集型洋中脊玄武岩; N-MORB. 正常型洋中脊玄武岩。数据据文献[38]。

图8 邵武地区玄武安山岩的球粒陨石标准化稀土元素配分曲线(a)和原始地幔标准化微量元素蛛网图(b)

Fig.8 Chondrite-normalized REE diagrams (a) and primitive mantle-normalized spider diagrams (b) of the basaltic andesite in the Shaowu area

表 4 邵武地区玄武安山岩的微量及稀土元素组成分析结果

Table 4 Trace element and REE contents of the basaltic andesite in the Shaowu area

样品号	Li	Sc	V	Ni	Co	Cu	Ga	Rb	Sr	Y	Zr	Nb	Cs	Ba	La
FJ11-6	103.99	19.90	157.40	9.62	24.84	8.24	15.82	62.17	187.92	15.79	95.93	9.49	4.72	277.11	15.08
FJ11-7	108.04	22.30	176.75	8.03	29.24	17.91	17.98	77.20	230.10	17.36	109.41	11.23	4.67	237.48	16.69
FJ11-8	98.20	20.99	163.41	8.46	27.07	16.02	16.61	76.84	279.05	16.78	103.20	10.25	4.49	328.29	15.46
FJ11-9	114.25	24.23	187.71	9.77	34.48	40.65	17.22	82.64	204.72	17.72	101.82	9.29	6.17	278.53	17.29
样品号	Ce	Pr	Nd	Sm	Eu	Gd	Tb	Dy	Ho	Er	Tm	Yb	Lu	Hf	Ta
FJ11-6	31.85	4.42	17.29	3.33	0.77	2.73	0.45	2.73	0.59	1.34	0.22	1.32	0.21	2.46	0.53
FJ11-7	35.93	4.95	19.35	3.61	0.85	2.99	0.50	3.01	0.64	1.52	0.24	1.40	0.25	2.84	0.62
FJ11-8	32.98	4.56	17.93	3.53	0.90	2.88	0.51	2.93	0.63	1.45	0.23	1.34	0.23	2.71	0.58
FJ11-9	35.48	4.95	19.33	3.75	0.86	2.91	0.50	3.12	0.68	1.59	0.26	1.42	0.26	2.68	0.47
样品号	Pb	Th	U	∑REE	LREE	HREE	LREE/HREE	(La/Yb) _N	(La/Sm) _N	(Gd/Yb) _N	Zr/Hf	δ Eu	δ Ce		
FJ11-6	7.16	3.34	1.14	82.33	72.74	9.59	7.59	7.69	2.85	1.66	40.19	0.76	0.93		
FJ11-7	6.96	3.83	1.39	91.94	81.38	10.55	7.71	8.02	2.91	1.72	38.75	0.77	0.94		
FJ11-8	7.38	3.58	1.32	85.57	75.36	10.21	7.38	7.77	2.75	1.73	37.59	0.84	0.94		
FJ11-9	9.11	3.82	1.08	92.40	81.66	10.74	7.60	8.21	2.90	1.65	35.85	0.77	0.91		

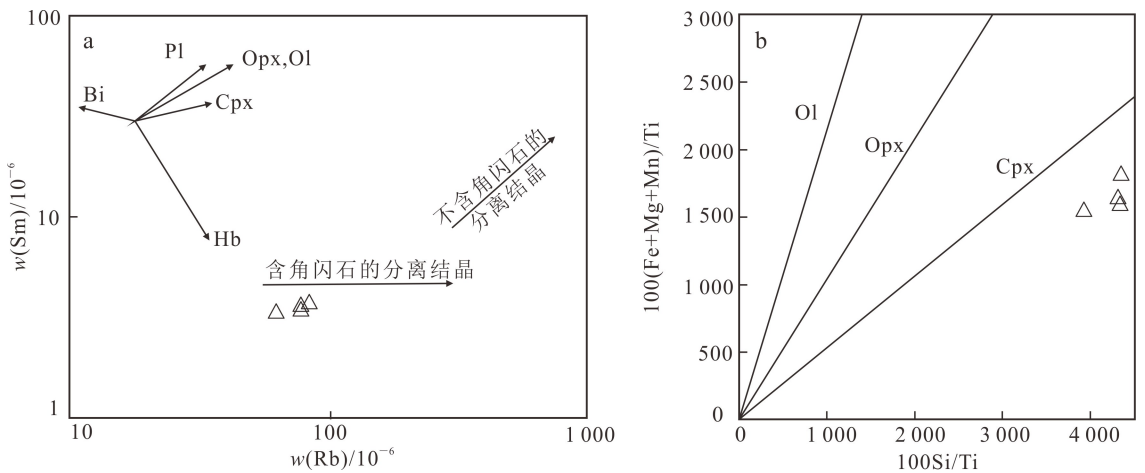
注:微量和稀土元素的质量分数单位为 10^{-6} 。

表 5 邵武地区玄武安山岩全岩 Sm - Nd 同位素组成

Table 5 Sm - Nd isotopic analyses for the basaltic andesite in the Shaowu area

样品编号	$w(\text{Sm})/10^{-6}$	$w(\text{Nd})/10^{-6}$	$^{147}\text{Sm}/^{144}\text{Nd}$	$^{143}\text{Nd}/^{144}\text{Nd}$	2σ	$(^{143}\text{Nd}/^{144}\text{Nd})_i$	$\epsilon_{\text{Nd}}(t)$	T_{DM}/Ma	T_{DM2}/Ma
FJ11-6	4.16	18.8	0.133 6	0.512 132	0.000 008	0.512 431	-8.6	1 940	1 650
FJ11-7	4.35	20.0	0.131 3	0.512 125	0.000 012	0.512 431	-8.7	1 900	1 660
FJ11-8	4.06	18.2	0.135 0	0.512 104	0.000 013	0.512 431	-9.2	2 020	1 670
FJ11-9	4.19	19.2	0.131 6	0.512 139	0.000 005	0.512 431	-8.4	1 890	1 640

注: T_{DM} 为模式年龄; T_{DM2} 为两阶段模式年龄。



Ol, 橄榄石; Opx, 斜方辉石; Cpx, 单斜辉石; Hb, 角闪石; Bi, 黑云母; Pl, 斜长石。

图 9 邵武地区玄武安山岩的 $w(\text{Sm})-w(\text{Rb})$ (a) 及 $100(\text{Fe}+\text{Mg}+\text{Mn})/\text{Ti}$ vs. $100\text{Si}/\text{Ti}$ (b) 图解

Fig.9 $w(\text{Sm})$ vs. $w(\text{Rb})$ (a) and $100(\text{Fe}+\text{Mg}+\text{Mn})/\text{Ti}$ vs. $100\text{Si}/\text{Ti}$ (b) diagram of the basaltic andesite in the Shaowu area

玄武安山岩的 Sm-Nd 同位素组成特征显示,它们具有较小的 $\epsilon_{\text{Nd}}(t)$ 值,从原始地幔标准化微量元素蛛网图(图 8b)中可见,样品显示出 Nb、Ta 强烈亏损, Pb 正异常和 Ti 弱负异常,造成这种特征的原因可能为:1)源区富集,即岩浆源区存在有因俯冲进入地幔的地壳物质组分;2)玄武安山岩在形成过程中受到了强烈的地壳物质混染。物质组成方面, Nb/Ta 值在岩浆形成之后基本上能够保持不变,对于反映岩浆源区有很好的指示意义。地壳物质相对于地幔熔体具有较低的 Nb、Ta 质量分数,较低的 Nb/Ta 值(地壳中 Nb/Ta = 8.33 ~ 13.33, 地幔中 Nb/Ta = 18.27^[49])和较高的 Th 质量分数;相比于原始岩浆,地壳混染后的岩浆具有较高的 Th/Nb (>5)和 Th/Ta (>10)值^[48],而样品中 Nb/Ta 值为 14.98 ~ 23.89, Th/Nb 和 Th/Ta 值分别为 0.30 ~ 0.41 和 5.40 ~ 8.15。据上述特征,认为邵武玄武安山岩岩浆并未表现出明显地壳混染的特征。另一方面,其他研究表明,高场强元素中 Zr/Hf 值对于岩浆源区的区分具有很好的指示意义,如地幔中 Zr/Hf 值约为 50,而地壳中 Zr/Hf 值约为 36^[50]。样品中 Zr/Hf 值为 38.85 ~ 40.19,指示邵武玄武安山岩的形成过程又涉及到一定壳源物质加入。岩浆上升过程中,无论是上地壳还是下地壳的混染,在造成岩浆 Pb 正异常的同时,均能够导致混染岩浆中 Ti 质量分数降低从而引起 Ti 的负异常^[51],样品中具有明显的 Pb 正异常和 Ti 负异常,表明有地壳物质的加入。稀土元素配分曲线图(图 8a)中,样品曲线与 OIB 曲线样式相似,但其微量元素中却表现为 Nb、Ta 负异常及 Pb 正异常等,显示出富集型地幔的特征。另外,玄武安山岩内部锆石 $\epsilon_{\text{Hf}}(t)$ 值为很小的负值,表明其源区主要来自古老的地壳物质。样品 $\epsilon_{\text{Hf}}(t)$ 和 $\epsilon_{\text{Nd}}(t)$ 均具有很小的负值,分别为 -14.33 ~ -8.98 和 -9.2 ~ -8.4,这在东南沿海地区的镁铁质火成岩是很少见的^[52]。相反地,这种情况在长英质岩石中较常见,如 Zhao 等^[53]获得了南岭地区晚侏罗世桃山花岗质岩石较低的 $\epsilon_{\text{Hf}}(t)$ (-14.3 ~ -4.8)和 $\epsilon_{\text{Nd}}(t)$ (-11.2 ~ -8.8)值,并根据地球化学特征认为它们源于古老变沉积岩的部分熔融。Li 等^[54]得出晚侏罗世佛冈岩基的 $\epsilon_{\text{Hf}}(t)$ 和 $\epsilon_{\text{Nd}}(t)$ 值分别为(-11.5 ~ -3.1)、(-12.2 ~ -4.3),属于古元古代中基性岩的部分熔融产物。刘高峰等^[55]报道了遂川晚侏罗世花岗岩 $\epsilon_{\text{Hf}}(t)$ 值为(-19.5 ~ -8.5),代表了深部热驱动下古老地壳熔

融的产物。类似的岩石在紫金山、汾山等其他地区也均有报道^[56-58]。华夏地块东部古老基底的 $\epsilon_{\text{Hf}}(t)$ 和 $\epsilon_{\text{Nd}}(t)$ 值分别在 < -10 和 $-16 \sim -8$ 。因此,结合本次研究得出的玄武安山岩 $\epsilon_{\text{Hf}}(t)$ 和 $\epsilon_{\text{Nd}}(t)$ 较小的负值,本文认为邵武玄武安山岩源区在发生部分熔融之前就已经发生了富集,幔源岩浆不断底侵到中、下地壳,破坏并置换了原有的老地壳,两者在源区发生相互作用,并通过部分熔融产生了母岩浆,同时也将古老地壳和地幔的部分地球化学信息传递到母岩中,随后通过演化形成了玄武安山岩。在岩浆演化和发展过程中并未经历明显的地壳混染。

4.3 大地构造意义

大量研究表明,在中—晚侏罗世,华南地区发生了挤压到板内伸展的构造体制转变^[11,54,59-60]。但对于具体构造转换的时间仍存在争议。Shi 等^[10]认为,随着俯冲角度的变化,构造背景从火山弧转变为中侏罗世(165 ~ 150 Ma)的弧后伸展,这对应着区域构造应力场从挤压向伸展的转变。余心起等^[61]通过沉积盆地研究,指出中国东南部早—中侏罗世普遍为拉张裂陷沉积环境,在泛滥平原环境中有裂陷型盆地共生。而其他学者^[6,10,12-17,45,47,62-110]认为伸展作用在晚侏罗世才开始,中侏罗世为挤压环境(表 6)。Su 等^[11]提出,晚侏罗世发生了有限的地幔上升流,暗示了从挤压到伸展的过渡阶段。Li 等^[112]指出,中—晚侏罗世太平洋板块持续北西向俯冲造成了大面积的挤压作用,在南岭地区发生了板片撕裂,形成了近 EW 向的裂谷带。舒良树^[27]也表示,在中侏罗世(190 ~ 160 Ma)期间东南沿海地区遭受了强烈挤压,此时南岭地区为拉张环境,主要发育双峰式火山岩、层状基性杂岩体、A 型花岗岩等。

邵武地区玄武安山岩具有高 Zr/Y、Th/Hf、Ta/Hf 值,在构造环境判别图中,主要位于板内玄武岩区和大陆拉张带(初始裂谷)玄武岩区(图 10),指示出玄武安山岩是在中侏罗世晚期(161.0 Ma)板块内部拉张环境下形成的。根据华南板块内火成岩地球化学的差异性及变化规律,古太平洋板块俯冲过程中,中生代经历了板片的回撤过程^[113-117],而不均一的板片后撤能够导致板片撕裂^[113,118-121],这就引发了明显的伸展作用,并导致软流圈物质上涌、底侵、置换华夏板块古老地壳物质,从而形成富集源区。

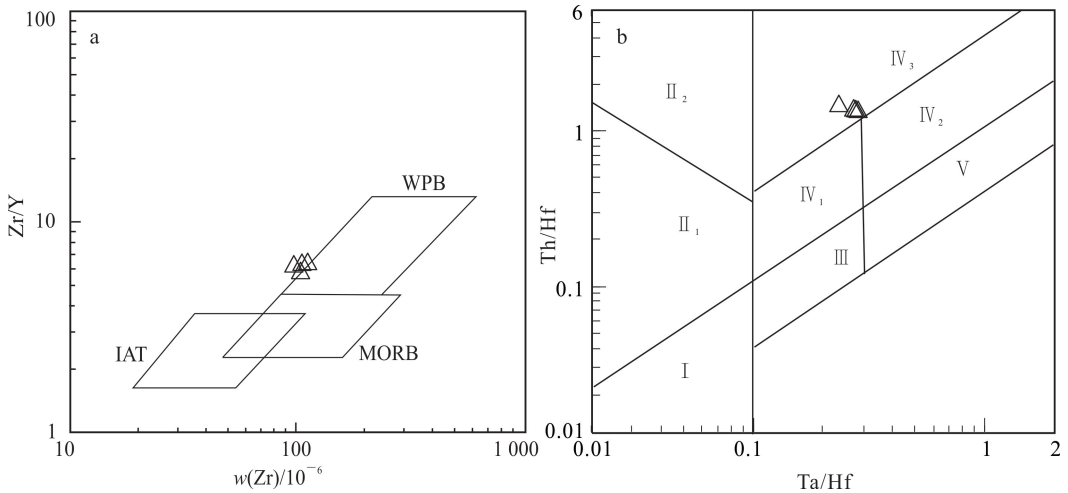
表 6 华南板块东部中侏罗世火山-侵入岩年龄及其地质背景

Table 6 List of ages of the Middle Jurassic volcanic-intrusive rocks in the eastern South China block

序号	位置	岩石类型	测试方法	地质背景	年龄/Ma	参考文献
1	浙江,梵音洞	石英闪长玢岩	LA-ICP-MS U-Pb 锆石	俯冲	169.8±1.1	[12]
2	浙江,绍兴	花岗闪长岩	LA-ICP-MS U-Pb 锆石	挤压	150.1±2.6	[62]
3	江西,德兴,富家坞	斑岩	LA-ICP-MS U-Pb 锆石	俯冲	171.7~171.0	[63]
4	江西,德兴	花岗闪长斑岩	LA-ICP-MS U-Pb 锆石	俯冲	171.0±3.0	[64]
5	浙江,松阳	流纹质玻屑凝灰岩	SHRIMP U-Pb 锆石	俯冲	153.0±2.0	[13]
6	浙江,毛弄	晶屑凝灰岩	SHRIMP U-Pb 锆石	俯冲	177.0±1.0	[44]
7	瓯江	花岗闪长岩	SHRIMP U-Pb 锆石	俯冲	174.4~173.7	[14]
8	浙江庆元	流纹质凝灰岩	LA-ICP-MS U-Pb 锆石	俯冲	176.0~169.1	[15]
9	江西,冷水坑	斑岩及晶屑凝灰岩	SHRIMP U-Pb 锆石	挤压	158.2~157.2	[45]
10	江西,天华山	流纹岩	LA-ICP-MS U-Pb 锆石	俯冲	159.4~151.6	[65]
11	福建,外屯	二长花岗岩	LA-ICP-MS U-Pb 锆石	俯冲	168.4±1.5	[47]
12	福建,余口	安山岩	SHRIMP U-Pb 锆石	挤压	162.3±3.7	[6]
13	福建,阔坑	花岗闪长岩	LA-ICP-MS U-Pb 锆石	俯冲	165.0~159.0	[66]
14	湖南,长城岭	玄武岩/玄武安山岩/粗面岩	⁴⁰ Ar- ³⁹ Ar 全岩	俯冲	178.0~170.0	[17]
15	福建,古田	花岗闪长斑岩	LA-ICP-MS U-Pb 锆石	岛弧	161.0~158.0	[67]
16	福建,紫金山	花岗岩	LA-ICP-MS U-Pb 锆石	俯冲	164.0~155.0	[67]
17	福建,福清	花岗岩/花岗闪长岩	LA-ICP-MS U-Pb 锆石	俯冲	187.0~130.0	[68]
18	台湾,大南澳	火山碎屑岩	SHRIMP U-Pb 锆石	俯冲	170.0	[69]
19	福建,东山	片麻状花岗岩	LA-ICP-MS U-Pb 锆石	弧相关	147.0~146.0	[70]
20	珠江口盆地	黑云母花岗岩	LA-ICP-MS U-Pb 锆石	火山弧	161.0~149.0	[10]
21	西沙	二长花岗岩和碱长花岗岩	LA-ICP-MS U-Pb 锆石	俯冲	158.0~144.0	[71]
22	南沙	斜长花岗岩/二长花岗岩	LA-ICP-MS U-Pb 锆石	汇聚	159.1~153.6	[16]
23	广山,浙江	钾长花岗岩	LA-ICP-MS U-Pb 锆石	拉伸	162.4~156.3	[72]
24	广山,浙江	花岗岩	LA-ICP-MS U-Pb 锆石	拉伸	147.2±1.7	[62]
25	曹娥,浙江	花岗斑岩	LA-ICP-MS U-Pb 锆石	拉伸	150.3±1.6	[73]
26	后山坞,浙江	花岗斑岩	LA-ICP-MS U-Pb 锆石	拉伸	149.1±1.1	[73]
27	金华,浙江	花岗斑岩,钾长花岗岩	LA-ICP-MS U-Pb 锆石	挤压向伸展过渡	150.6~144.0	[74]
28	丽水,浙江	流纹质玻屑凝灰岩	SHRIMP/ LA-ICP-MS U-Pb 锆石	挤压向伸展 过渡	155.0~152.0	[75]
29	冷水坑,江西	花岗斑岩	LA-ICP-MS U-Pb 锆石	伸展	163.6~154.3	[76]
30	冷水坑,江西	流纹质晶屑熔结凝灰岩	LA-ICP-MS U-Pb 锆石	伸展	160.8~146.6	[76]
31	大冶,湖北	闪长岩	SHRIMP U-Pb 锆石	伸展	151.8±2.8	[77]
32	城门山,江西	花岗斑岩	SIMS U-Pb 锆石	挤压向伸展过渡	146.0~144.5	[78]
33	浒坑,江西	白云母花岗岩	LA-ICP-MS U-Pb 锆石	伸展	152.0±2.6	[79]
34	武功山,江西	花岗岩	LA-ICP-MS U-Pb 锆石	伸展	158.0~154.0	[80]
35	水口山,湖南	花岗闪长斑岩	SHRIMP 锆石 U-Pb	伸展	155.5±1.7	[81]
36	九嶷山,湖南	花岗岩	SHRIMP U-Pb 锆石	伸展	157.0~156.0	[82]
37	锡山,湖南	花岗岩	SHRIMP U-Pb 锆石	伸展	156.0±2.0	[83]
38	宝山,湖南	花岗闪长斑岩	SHRIMP 锆石 U-Pb	伸展	158.0±2.0	[84]
39	宝山,湖南	花岗闪长斑岩	LA-ICP-MS U-Pb 锆石	伸展	157.0~154.0	[85]
40	黄沙坪,湖南	英安斑岩、石英斑岩、 二长花岗岩	LA-ICP-MS U-Pb 锆石	伸展	160.0~155.0	[86]
41	骑田岭,湖南	黑云母花岗闪长岩	TIMS U-Pb 锆石	伸展	161.0±2.0	[87]
42	九峰,广东	黑云母花岗岩	LA-ICP-MS U-Pb 锆石	伸展	160.2±1.3	[88]

续表 6

序号	位置	岩石类型	测试方法	地质背景	年龄/Ma	参考文献
43	九峰广东	花岗岩	SIMS U - Pb 锆石	伸展	159.7~156.8	[89]
44	淘锡坑,江西	花岗岩	SHRIMP U - Pb 锆石	伸展	158.7~157.6	[90]
45	漂塘,江西	黑云母花岗岩	TIMS U - Pb 锆石	伸展	162.0~153.0	[91]
46	天门山,江西	黑云母花岗岩、花岗斑岩	SHRIMP 锆石 U - Pb	伸展	152.0~151.0	[92]
47	张天塘,江西	白云母花岗岩	SHRIMP 锆石 U - Pb	伸展	157.0±1.7	[93]
48	大吉山,江西	白云母花岗岩	TIMS U - Pb 锆石	伸展减薄	152.0±1.6	[94]
49	全南,江西	正长岩	SHRIMP U - Pb 锆石	伸展	161.0±4.0	[95]
50	武平,福建	黑云母花岗岩	LA - ICP - MS U - Pb 锆石	伸展	161.4	[96]
51	古田,福建	黑云母二长花岗岩	ELA - ICP - MS U - Pb 锆石	伸展	161.0±1.0	[97]
52	大东山,广东	花岗岩	SHRIMP U - Pb 锆石	伸展	165.0~159.0	[98]
53	桂洞,广东	黑云母花岗岩、二云母花岗岩	LA - ICP - MS U - Pb 锆石	伸展	160.0~151.0	[99]
54	紫金山,福建	花岗岩	SIMS U - Pb 锆石	构造伸展	157.6±1.9	[100]
55	才溪,福建	二长花岗岩	SHRIMP U - Pb 锆石	挤压向伸展过渡	150.0±3.0	[101]
56	湘南-桂东	玄武岩、正长岩	Ar - Ar	伸展	175.0~150.0	[102]
57	里松,广西	黑云母花岗岩	SIMS U - Pb 锆石	伸展	160.0±1.0	[103]
58	姑婆山,广西	闪长岩、石英二长岩、 黑云母花岗岩	SHRIMP/TIMS/ LA - ICP - MS U - Pb 锆石	伸展	163.0~151.0	[104]
59	姑婆山,广西	花岗岩	LA - ICP - MS U - Pb 锆石	伸展	162.0	[105]
60	佛冈,广东	花岗岩	SHRIMP U - Pb 锆石	伸展	165.0~158.0	[106]
61	乌石,广东	闪长岩	LA - ICP - MS U - Pb 锆石	伸展	162.3±1.3	[107]
62	河源,广东	花岗岩	TIMS U - Pb 锆石	伸展	149.0±1.6	[108]
63	清湖,广东	二长花岗岩	SIMS U - Pb 锆石	伸展	160.0±1.0	[103]
64	五桂山,广东	花岗闪长岩、黑云母花岗岩	SIMS U - Pb 锆石	板内伸展	166.0~159.0	[109]
65	香港	晶屑凝灰岩、流纹岩	TIMS U - Pb 锆石	伸展	147.5~142.7	[110]



WPB. 板内; MORB. 大洋中脊; IAT. 岛弧。I. N - MORB 区; II₁. 大洋岛弧玄武岩区; II₂. 陆缘岛弧及陆缘火山弧玄武岩区; III. 大洋板内洋岛、海山玄武岩及过渡/富集大洋中脊玄武岩区; IV₁. 陆内裂谷及陆缘裂谷拉斑玄武岩区; IV₂. 陆内裂谷碱性玄武岩区; IV₃. 大陆拉张带(初始裂谷)玄武岩区; V. 地幔热柱玄武岩区。

图 10 邵武地区玄武安山岩 Zr/Y - w(Zr) (a) 和 Th/Hf - Ta/Hf (b) 图解

Fig.10 Zr/Y vs. w(Zr) (a) and Th/Hf vs. Ta/Hf (b) diagrams of the basaltic andesite in the Shaowu area

结合前人研究成果,本文支持研究区在中侏罗世晚期属于拉张环境的观点,即区域伸展作用在中侏罗世晚期已经有所体现。但另一方面,构造地质学^[11]、沉积学^[26]、岩石学^[13,122]等证据显示出中侏罗世东南沿海发育强烈的挤压应力场,结合前人数据及本次研究结果,认为该地区属于整体挤压背景下的局部伸展环境。邢光福等^[6]指出中—晚侏罗世华南处于挤压还是拉张环境这一争议的原因在于,火山岩主要沿张性断裂上升侵位或喷发,但这种张性断裂有可能是区域整体挤压背景下局部存在拉张;基于金华地区花岗岩类的地球化学分析,高万里^[74]指出由于古太平洋板块俯冲的后退,华南板块经历了从整体挤压和局部伸展背景(中侏罗世)到大规模伸展背景(晚侏罗世)的转变。因此,本文认为邵武地区火山作用发生于板内伸展,表明中侏罗世晚期在东南沿海的俯冲的背景下仍局部存在伸展环境,这源于板块回撤引发的拉伸,同时也诱发了俯冲带深部地幔物质与地壳的混合、置换等作用。

5 结论

1) LA-ICP-MS 锆石 U-Pb 同位素定年结果表明,邵武地区玄武安山岩形成时代为中侏罗世晚期(161.0 ± 2.0 Ma),指示出闽北地区存在中侏罗世晚期的一期岩浆作用。

2) 邵武地区玄武安山岩为钙碱性玄武岩,岩石富集轻稀土及大离子亲石元素 Rb、Ba 和 K,高场强元素 Nb、Ta、Ti 和 P 相对亏损。地球化学特征指示其母岩浆应是由拉张环境下的富集型岩石圈地幔部分熔融产生,经历一定结晶分异作用,其地壳混染作用不明显。

3) 邵武地区玄武安山岩指示中侏罗世晚期东南沿海地区俯冲背景下,板片发生回撤导致局部拉张。

参考文献 (References):

- [1] 路凤香,桑隆康.岩石学[M].北京:地质出版社,2002.
Lu Fengxiang, Sang Longkang. Petrology [M]. Beijing: Geological Publishing House, 2002.
- [2] Bowen N L. The Evolution of the Igneous Rocks[M]. New York: Princeton University Press, 1928.
- [3] 王强,赵振华,许继峰,等.天山北部石炭纪埃达克岩-高镁安山岩-富 Nb 岛弧玄武质岩:对中亚造山带显生宙地壳增生与铜金成矿的意义[J].岩石学报,2006,22(1):11-30.
Wang Qiang, Zhao Zhenhua, Xu Jifeng, et al. Carboniferous Dakite-High-Mg Andesite - Nb - Enriched Basaltic Rock in the Northern Tianshan: Implications for Phanerozoic Crustal Growth in the Central Asian Orogenic Belt and Cu - Au Mineralization[J]. Acta Petrologica Sinica, 2006, 22(1): 11 - 30.
- [4] 赵子福,代富强,陈启.大陆板片-地幔相互作用:来自大别造山带碰撞后安山质火山岩的地球化学证据[J].地球科学,2019,44(12):4119-4127.
Zhao Zifu, Dai Fuqiang, Chen Qi. Continental Slab-Mantle Interaction: Geochemical Evidence from Post-Collisional Andesitic Rocks in the Dabie Orogen[J]. Earth Science, 2019, 44(12): 4119 - 4127.
- [5] 娄元林,唐饶,李毅,等.西藏古堆地区岩浆岩基本特征及对成矿的响应[J].黄金,2022,43(1):20-27.
Lou Yuanlin, Tang Yao, Li Yi, et al. Fundamental Characteristics and Metallogenic Response of the Magmatic Rocks in Gudui Area, Tibet[J]. Gold, 2022, 43(1): 20 - 27.
- [6] 邢光福,卢清地,陈荣,等.华南晚中生代构造体制转折结束时限研究:兼与华北燕山地区对比[J].地质学报,2008,82(4):451-463.
Xing Guangfu, Lu Qingdi, Chen Rong, et al. Study on the Ending Time of Late Mesozoic Tectonic Regime Transition in South China: Comparing to the Yanshan Area in North China[J]. Acta Geologica Sinica, 2008, 82(4): 451 - 463.
- [7] Mao J W, Cheng Y B, Chen M H, et al. Major Types and Time-Space Distribution of Mesozoic Ore Deposits in South China and Their Geodynamic Settings[J]. Mineralium Deposita, 2013, 48: 267 - 294.
- [8] 彭松柏,刘松峰,林木森,等.华夏早古生代俯冲作用 II: 大夹高镁-镁质安山岩新证据[J].地球科学,2016,41(6):931-947.
Peng Songbai, Liu Songfeng, Lin Musen, et al. Early Paleozoic Subduction in Cathaysia II: New Evidence for the Dashuang High Magnesian-Magnesian Andesite [J]. Earth Science, 2016, 41(6): 931 - 947.
- [9] 陈毓川,王登红,徐志刚,等.中国重要矿产和区域成矿规律[M].北京:地质出版社,2015.
Chen Yuchuan, Wang Denghong, Xu Zhigang, et al. Important Mineral and Regularity in China [M]. Beijing: Geological Publishing House, 2015.
- [10] Shi H S, Xu C H, Zhou Z Y, et al. Zircon U - Pb Dating on Granitoids from the Northern South China Sea and Its Geotectonic Relevance[J]. Acta Geologica Sinica, 2011, 85(6): 1359 - 1372.

- [11] 张岳桥,董树文,李建华,等.华南中生代大地构造研究新进展[J].地球学报,2012,33(3):257-279.
Zhang Yueqiao, Dong Shuwen, Li Jianhua, et al. The New Progress in the Study of Mesozoic Tectonics of South China[J]. Acta Geoscientica Sinica, 2012, 33(3): 257-279.
- [12] Zhao J L, Qiu J S, Liu L. Early-Middle Jurassic Magmatic Rocks Along the Coastal Region of Southeastern China: Petrogenesis and Implications for Paleo-Pacific Plate Subduction [J]. Journal of Asian Earth Sciences, 2021, 210(1): 104687.
- [13] 张伟,吴鸿翔,朱孔阳,等.华南东部陆缘侏罗纪岩浆作用特征及其构造背景:来自浙东南毛弄组火山岩的新证据[J].岩石学报,2018,34(11):3375-3398.
Zhang Wei, Wu Hongxiang, Zhu Kongyang, et al. The Jurassic Magmatism and Its Tectonic Setting in the Eastern Margin of South China: Evidence from the Volcanic Rocks of the Maonong Formation in the SE Zhejiang [J]. Acta Petrologica Sinica, 2018, 34(11): 3375-3398.
- [14] Yuan W, Yang Z Y, Zhao X X, et al. Early Jurassic Granitoids from Deep Drill Holes in the East China Sea Basin: Implications for the Initiation of Palaeo-Pacific Tectono-Magmatic Cycle [J]. International Geology Review, 2018, 60(7): 813-824.
- [15] 邢新龙.浙闽交界地区侏罗纪-白垩纪火山活动年代学与岩石成因研究[D].成都:成都理工大学,2016.
Xing Xinlong. Chronology and Petrogenesis of Jurassic-Cretaceous Volcanism in the Area of Zhejiang-Fujian Boundary [D]. Chengdu: Chengdu University of Technology, 2016.
- [16] Yan Q S, Shi X F, Liu J H, et al. Petrology and Geochemistry of Mesozoic Granitic Rocks from the Nansha Micro-Block, the South China Sea: Constraints on the Basement Nature [J]. Journal of Asian Earth Sciences, 2010, 37(2): 130-139.
- [17] Jiang Y H, Jiang S Y, Dai B Z, et al. Middle to Late Jurassic Felsic and Mafic Magmatism in Southern Hunan Province, Southeast China: Implications for a Continental Arc to Rifting [J]. Lithos, 2009, 107: 185-204.
- [18] Chen J F, Foland K A, Xing F M, et al. Magmatism Along the Southeast Margin of the Yangtze Block: Precambrian Collision of the Yangtze and Cathaysia Blocks of China [J]. Geology, 1991, 19: 815-818.
- [19] Charvet J. The Neoproterozoic-First Paleozoic Tectonic Evolution of the South China Block: An Overview [J]. Asian Earth Sci, 2013, 74: 198-209.
- [20] Li J H, A Cawood P, Ratschbacher L, et al. Building Southeast China in the Late Mesozoic: Insights from Alternating Episodes of Shortening and Extension Along the Lianhuashan Fault Zone [J]. Earth-Science Reviews, 2020, 201: 103056.
- [21] Shu L S, Yao J L, Wang B, et al. Neoproterozoic Plate Tectonic Process and Phanerozoic Geodynamic Evolution of the South China Block [J]. Earth-Science Review, 2021, 216: 103596.
- [22] Maruyama S. Pacific-Type Orogeny Revisited: Miyashiro-Type Orogeny Proposed [J]. Island Arc, 1997, 6: 91-120.
- [23] Shu L S, Wang B, Cawood P A, et al. Early Paleozoic and Early Mesozoic Intraplate Tectonic and Magmatic Events in the Cathaysia Block, South China [J]. Tectonics, 2015, 34: 1600-1621.
- [24] 段政,刑光福,余明刚,等.东南沿海早白垩世火山岩的极低级变质作用研究 [J]. 岩石学报, 2018, 34(3): 656-668.
Duan Zheng, Xing Guangfu, Yu Minggang, et al. Very Low-Grade Metamorphism of Early Cretaceous Volcanic Rocks in the Southeast Coastal of China [J]. Acta Petrologica Sinica, 2018, 34(3): 656-668.
- [25] 李三忠,李玺瑶,赵淑娟,等.全球早古生代造山带: III: 华南陆内造山 [J]. 吉林大学学报(地球科学版), 2016, 46(4): 1005-1025.
Li Sanzhong, Li Xiyao, Zhao Shujuan, et al. Global Early Paleozoic Orogenic Belt: III: Intracontinental Orogenic in South China [J]. Journal of Jilin University (Earth Science Edition), 2016, 46(4): 1005-1025.
- [26] 薛怀民,马芳,宋永勤,等.江南造山带东段新元古代花岗岩组合的年代学和地球化学:对扬子与华夏地块拼合时间与过程的约束 [J]. 岩石学报, 2010, 26(11): 3215-3244.
Xue Huaimin, Ma Fang, Song Yongqin, et al. Geochronology and Geochemistry of the Neoproterozoic Granitoid Association from Eastern Segment of the Jiangnan Orogen China: Constraints on the Time and Process of Amalgamation Between the Yangtze and Cathaysia Blocks [J]. Acta Petrologica Sinica, 2010, 26(11): 3215-3244.
- [27] 舒良树.华南构造演化的基本特征 [J]. 地质通报, 2012, 31(7): 1035-1053.
Shu Liangshu. An Analysis of Principal Features of

- Tectonic Evolution in South China Block [J]. Geological Bulletin of China, 2012, 31(7): 1035 - 1053.
- [28] 陈正宏,李寄嵎,谢佩珊,等.利用 EMP 独居石定年法探讨浙闽武夷山地区变质基底岩石与花岗岩的年龄[J].高校地质学报,2008,14(1):1-15.
Chen Zhenghong, Li Jiyu, Xie Peishan, et al. Approaching the Age Problem for Some Metamorphosed Precambrian Basement Rocks and Phanerozoic Granitic Bodies in the Wuyishan Area: The Application of EMP Monazite Age Dating[J]. Geological Journal of China Universities, 2008, 14(1): 1-15.
- [29] Yu J H, O'Reilly S Y, Zhou M F, et al. U - Pb Geochronology and Hf - Nd Isotopic Geochemistry of the Badu Complex, Southeastern China; Implications for the Precambrian Crustal Evolution and Paleogeography of the Cathaysia Block [J]. Precambrian Research, 2012, 222/223: 424 - 449.
- [30] 福建省 713 地质队.1 : 20 万顺层幅地质图及说明书[R].福州:福建省地质调查局,1971.
Fujian Province 713 Geological Team. 1 : 200 000 Along the Strata Geological Map and Description[R]. Fuzhou: Fujian Provincial Geological Survey, 1971.
- [31] Hou K J, Li Y H, Tian Y Y. In Situ U - Pb Zircon Dating Using Laser Ablation-Multi Ion Counting-ICP-MS[J]. Mine Depos, 2009, 28: 481 - 492.
- [32] Wang Y X, Yang J D, Chen J, et al. The Sr and Nd Isotopic Variations of the Chinese Loess Plateau During the Past 7 Ma; Implications for the East Asian Winter Monsoon and Source Areas of Loess [J]. Palaeogeography, Palaeoclimatology, Palaeoecology, 2007, 249(3/4): 351 - 361.
- [33] Lapiere H, Bosch D, Narros A, et al. The Mamonia Complex (SW Cyprus) Revisited; Remnant of Late Triassic Intra-Oceanic Volcanism Along the Tethyan Southwestern Passive Margin [J]. Geological Magazine, 2007, 144(1): 1 - 9.
- [34] 王硕,李志谦,刘云华,等.延边赤卫沟金矿床成矿物质来源及成矿机制研究[J].黄金,2023,44(2):60-66.
Wang Shou, Li Zhiqian, Liu Yunhua, et al. Sources of Metallogenic Materials and Metallogenic Mechanism of Chiweiguo Gold Deposit, Yanbian[J]. Gold, 2023, 44(2): 60 - 66.
- [35] Hastie A R, Kerr A C, Pearce J A, et al. Using Immobile Trace Elements: Development of the Th-Co Discrimination Diagram [J]. Journal of Petrology, 2007, 48(12): 2341 - 2357.
- [36] Winchester J A, Floyd P A. Geochemical Discrimination of Different Magma Series and Their Differentiation Products Using Immobile Elements [J]. Chemical Geology, 1977, 20: 325 - 343.
- [37] 王俊德,汤立伟,杜庆安,等.福建吉花金银矿床地质特征及含矿蚀变带元素迁移对区域成矿的启示[J].黄金,2024,45(3):55-66.
Wang Junde, Tang Liwei, Du Qing'an, et al. Geological Characteristics of Jihua Gold-Silver Deposit in Fujian and Implications of Element Migration in the Ore-Bearing Alteration Zone for Regional Mineralization[J]. Gold, 2024, 45(3): 55 - 66.
- [38] Sun S S, McDonough W F. Chemical and Isotopic Systematics of Oceanic Basalts: Implications for Mantle Composition and Processes [J]. Geological Society, London, Special Publications, 1989, 42(1): 313 - 345.
- [39] Jacobson S B, Wasserburg G J. Sm - Nd Isotopic Evolution of Chondrites [J]. Earth and Planetary Science Letters, 1980, 50(1): 139 - 155.
- [40] 朱玉麟,张金塔.对福建西部早古生代地层划分及对比问题的商榷[J].福建地质,1988,7:142-161.
Zhu Yulin, Zhang Jinta. A Discussion on the Classification and Correlation of the Early Palaeozoic Strata in Western Fujian Province [J]. Geology of Fujian, 1988, 7: 142 - 161.
- [41] 舒良树.华南前泥盆纪构造演化:从华夏地块到加里东期造山带[J].高校地质学报,2006,12(4):418-431.
Shu Liangshu. Predevonian Tectonic Evolution of South China: From Cathaysian Block to Caledonian Period Folded Orogenic Belt[J]. Geological Journal of China Universities, 2006, 12(4): 418 - 431.
- [42] Wang D S, Li J W, She H Q, et al. Late Jurassic Volcanism Deduced from Geochemical, Geochronological, and Sr - Nd - Hf Isotopic Composition Characteristics of the Nanyuan Formation, South China[J]. Acta Geologica Sinica, 2023, 97(2): 449 - 468.
- [43] Chen P R, Hua R M, Zhang B T, et al. Early Yanshanian Post-Orogenic Granitoids in the Nanling Region - Petrological Constraints and Geodynamic Settings[J]. Science in China (Series D), 2002, 45

- (8): 755 - 768.
- [44] Liu L, Xu X S, Zou H B. Episodic Eruptions of the Late Mesozoic Volcanic Sequences in Southeastern Zhejiang, SE China: Petrogenesis and Implications for the Geodynamics of Paleo-Pacific Subduction[J]. *Lithos*, 2012, 154: 166 - 180.
- [45] 孟祥金,徐文艺,杨竹森,等.江西冷水坑矿田火山-岩浆活动时限:SHRIMP 锆石 U-Pb 年龄证据[J]. *矿床地质*, 2012, 31(4): 831 - 838.
- Meng Xiangjin, Xu Wenyi, Yang Zhusen, et al. Time Limit of Volcanic-Magmatic Action in Lengshuikeng Orefield, Jiangxi: Evidence from SHRIMP Zircon U-Pb Ages[J]. *Mineral Deposits*, 2012, 31(4): 831 - 838.
- [46] 邱骏挺,余心起,吴淦国,等.江西冷水坑矿区构造-岩浆活动的年代学约束[J]. *岩石学报*, 2013, 29(3): 812 - 826.
- Qiu Junting, Yu Xinqi, Wu Ganguo, et al. Geochronology of Igneous Rocks and Nappe Structures in Lengshuikeng Deposit, Jiangxi Province, China[J]. *Acta Petrologica Sinica*, 2013, 29(3): 812 - 826.
- [47] Wang G C, Jiang Y H, Liu Z, et al. Multiple Origins for the Middle Jurassic to Early Cretaceous High-K Calc-Alkaline I-Type Granites in Northwestern Fujian Province, SE China and Tectonic Implications[J]. *Lithos*, 2016, 246/247: 197 - 211.
- [48] Neal C R, Mahoney J J, Chazey W J. Mantle Sources and the Highly Variable Role of Continental Lithosphere in Basalt Petrogenesis of the Kerguelen Plateau and Broken Ridge LIP: Results from ODP Leg 183 [J]. *Journal of Petrology*, 2002, 43(7): 1177 - 1205.
- [49] Hofmann A W. Chemical Differentiation of the Earth: The Relationship Between Mantle, Continental Crust, and Oceanic Crust[J]. *Earth and Planetary Science Letters*, 1988, 90(3): 297 - 314.
- [50] Anderson D L. Chemical Composition of the Mantle *Journal of Geophysical Research* [J]. *Solid Earth*, 1983, 88(Sup.1): 41 - 52.
- [51] 秦社彩,范蔚茗,郭锋.江绍断裂带晚中生代镁铁质火山岩成因及其深部过程意义[J]. *岩石学报*, 2019, 35(6): 1892 - 1906.
- Qin Shecai, Fan Weiming, Guo Feng. Petrogenesis and Geodynamic Implications of Late Mesozoic Mafic Volcanic Rocks Along the Jiangshan-Shaoxing Fault in SE China[J]. *Acta Petrologica Sinica*, 2019, 35(6): 1892 - 1906.
- [52] 缪柏虎,徐兆文,王浩,等.山东邹平青山下亚组玄武安山岩源区性质及成因[J]. *地质学报*, 2015, 89(1): 37 - 48.
- Miao Bohu, Xu Zhaowen, Wang Hao, et al. Genesis and Source Characteristic of Basaltic Andesite for Lower Qinshan Formation in Zouping Volcanic Basin, Shandong Province[J]. *Acta Geologica Sinica*, 2015, 89(1): 37 - 48.
- [53] Zhao Z F, Gao P, Zheng Y F. The Source of Mesozoic Granitoids in South China: Integrated Geochemical Constraints from the Taoshan Batholith in the Nanling Range [J]. *Chem Geol*, 2015, 395: 11 - 26.
- [54] Li X H, Li Z X, Li W X, et al. U-Pb Zircon, Geochemical and Sr-Nd-Hf Isotopic Constraints on Age and Origin of Jurassic I-and A-Type Granites from Central Guangdong, SE China: A Major Igneous Event in Response to Foundering of a Subducted Flat-Slab? [J]. *Lithos*, 2007, 96(1/2): 186 - 204.
- [55] 刘高峰,王连训,罗春林,等.赣南遂川晚侏罗世幕式花岗岩岩浆活动:年代学、地球化学和 Lu-Hf 同位素约束[J]. *岩石学报*, 2023, 39(8): 2489 - 2510.
- Liu Gaofeng, Wang Lianxun, Luo Chunlin, et al. Late Jurassic Episodic Granitic Magmatism in Suichuan, Southern Jiangxi: Constraints from Chronology, Geochemistry and Lu-Hf Isotope [J]. *Acta Petrologica Sinica*, 2023, 39(8): 2489 - 2510.
- [56] Jiang S H, Liang Q L, Bagas L, et al. Geodynamic Setting of the Zijinshan Porphyry-Epithermal Cu-Au-Mo-Ag Ore System, SW Fujian Province, China: Constrains from the Geochronology and Geochemistry of the Igneous Rocks [J]. *Ore Geology Reviews*, 2013, 53: 287 - 305.
- [57] Ding X, Sun W D, Chen W F, et al. Multiple Mesozoic Magma Processes Formed the 240 - 185 Ma Composite Weishan Pluton, South China: Evidence from Geochronology, Geochemistry, and Sr-Nd Isotopes [J]. *International Geology Review*, 2015, 57(9/10): 1189 - 1217.
- [58] Xu X B. Late Triassic to Middle Jurassic Tectonic Evolution of the South China Block: Geodynamic Transition from the Paleo-Tethys to the Paleo-Pacific Regimes [J]. *Earth-Science Reviews*, 2023, 241: 104404.
- [59] 陈培荣,周新民,张文兰,等.南岭东段燕山早期正长

- 岩-花岗岩杂岩的成因和意义[J].中国科学(D辑), 2004, 34(6): 493 - 503.
- Chen Peirong, Zhou Xinmin, Zhang Wenlan, et al. The Origin and Significance of Early Syenite-Granite Hybrid Rocks in the Eastern Section of Nanling[J]. Sciences in China (Series D), 2004, 34(6): 493 - 503.
- [60] Zhou X M, Sun T, Shen W Z, et al. Petrogenesis of Mesozoic Granitoids and Volcanic Rocks in South China: A Response to Tectonic Evolution [J]. Episodes, 2006, 29(1): 26 - 33.
- [61] 余心起, 舒良树, 邓平, 等. 中国东南部侏罗纪—第三纪陆相地层沉积特征[J]. 地层学杂志, 2003, 27(3): 254 - 263.
- Yu Xinqi, Shu Liangshu, Deng Ping, et al. The Sedimentary Features of the Jurassic-Tertiary Terrestrial Strata in Southeast China[J]. Journal of Stratigraphy, 2003, 27(3): 254 - 263.
- [62] 张建芳, 解怀生, 许兴苗, 等. 浙江漓渚地区栅溪—广山岩体地质地球化学特征、构造及找矿意义[J]. 中国地质, 2013, 40(2): 403 - 413.
- Zhang Jianfang, Xie Huaisheng, Xu Xingmiao, et al. Geological and Geochemical Characteristics and Tectonic and Prospecting Significance of the Shanxi-Guangshan Intrusions in Lizhu Area, Zhejiang Province[J]. Geology in China, 2013, 40(2): 403 - 413.
- [63] Zhou Q, Jiang Y H, Zhao P, et al. Origin of the Dexing Cu - Bearing Porphyries, SE China: Elemental and Sr - Nd - Pb - Hf Isotopic Constraints [J]. International Geology Review, 2012, 54, 572 - 592.
- [64] 郭博然, 刘树文, 杨朋涛, 等. 江西卧龙谷花岗岩和铜厂花岗岩闪长斑岩的地球化学特征及成因: 对赣东北地区铜矿成矿地质背景的制约[J]. 地质通报, 2013, 32(7): 1035 - 1046.
- Guo Boran, Liu Shuwen, Yang Pengtao, et al. Petrology, Geochemistry and Petrogenesis of Wolonggu Granites and Tongchang Granodioritic Porphyries: Constraints on Copper Metallogenic Geological Settings in Northeastern Jiangxi Province [J]. Geological Bulletin of China, 2013, 32(7): 1035 - 1046.
- [65] Yan X, Jiang S Y, Jiang Y H. Geochronology, Geochemistry and Tectonic Significance of the Late Mesozoic Volcanic Sequences in the Northern Wuyi Mountain Volcanic Belt of South China[J]. Gondwana Research, 2016, 37: 362 - 383.
- [66] Li Y, Ma C Q, Xing G F, et al. Origin of a Cretaceous Low - O - 18 Granitoid Complex in the Active Continental Margin of SE China[J]. Lithos, 2015, 216/217: 136 - 147.
- [67] Li B, Jiang S Y, Lu A H, et al. Petrogenesis of Late Jurassic Granodiorites from Gutian, Fujian Province, South China: Implications for Multiple Magma Sources and Origin of Porphyry Cu - Mo Mineralization[J]. Lithos, 2016, 264: 540 - 554.
- [68] 刘潜, 于津海, 苏斌, 等. 福建锦城 187 Ma 花岗岩的发现: 对华南沿海早侏罗世构造演化的制约[J]. 岩石学报, 2011, 27(12): 3575 - 3589.
- Liu Qian, Yu Jinhai, Su Bin, et al. Discovery of the 187 Ma Granite in Jincheng Area, Fujian Province: Constraint on Early Jurassic Tectonic Evolution of Southeastern China[J]. Acta Petrologica Sinica, 2011, 27(12): 3575 - 3589.
- [69] Li Z, Qiu J S, Xu X S. Geochronological, Geochemical and Sr - Nd - Hf Isotopic Constraints on Petrogenesis of Late Mesozoic Gabbro-Granite Complexes on the Southeast Coast of Fujian, South China: Insights into a Depleted Mantle Source Region and Crust-Mantle Interactions [J]. Geological Magazine, 2012, 149(3): 459 - 482.
- [70] Liu Q, Yu J H, Wang Q, et al. Ages and Geochemistry of Granites in the Pingtan-Dongshan Metamorphic Belt, Coastal South China: New Constraints on Late Mesozoic Magmatic Evolution [J]. Lithos, 2012, 150: 268 - 286.
- [71] 修淳, 张道军, 翟世奎, 等. 西沙岛礁基底花岗质岩石的锆石 U - Pb 年龄及其地质意义[J]. 海洋地质与第四纪地质, 2016, 36(3): 115 - 126.
- Xiu Chun, Zhang Daojun, Zhai Shikui, et al. Zircon U - Pb Age of Granitic Rocks from the Basement Beneath the Shi Island, Xisha Islands and Its Geological Significance [J]. Marine Geology & Quaternary Geology, 2016, 36(3): 115 - 126.
- [72] Jia D L, Yan G S, Ye T Z, et al. Zircon U - Pb Dating, Hf Isotopic Compositions and Petrochemistry of the Guangshan Granitic Complex in Shaoxing Area of Zhejiang Province and Its Geological Significance[J]. Acta Petrologica Sinica, 2013, 29(12): 4087 - 4103.
- [73] Wang D X, Gao W L, Li C L, et al. LA - ICP - MS Zircon U - Pb Geochronology, Petrochemistry of the Late Jurassic Granite Porphyry in Central Zhejiang

- Province and Their Geological Significance [J]. *Geology in China*, 2015, 42(6): 1684-1699.
- [74] 高万里. 浙东南中生代岩浆活动及其构造背景研究[D]. 北京: 中国地质科学院, 2014.
- Gao Wanli. Research of Mesozoic Magmatism and Tectonic Setting in Southeast Zhejiang Province[D]. Beijing: Chinese Academy of Geological Sciences, 2014.
- [75] Wang J E, Liu Y D, Wang J G, et al. Age Assignment of the Moshishan Group Volcanic Rocks in the Lishui Area, Zhejiang Province[J]. *East China Geology*, 2016, 37(3): 157-165.
- [76] Qiu J T, Yu X Q, Wu G G, et al. Geochronology of Igneous Rocks and Nappe Structures in Lengshuikeng Deposit, Jiangxi Province, China[J]. *Acta Petrologica Sinica*, 2013, 29(3): 812-838.
- [77] Li J W, Zhao X F, Zhou M F, et al. Late Mesozoic Magmatism from the Daye Region, Eastern China: U-Pb Ages, Petrogenesis, and Geodynamic Implications[J]. *Contributions to Mineralogy and Petrology*, 2009, 157: 383-409.
- [78] Li X H, Li W X, Wang X C, et al. SIMS U-Pb Zircon Geochronology of Porphyry Cu-Au-(Mo) Deposits in the Yangtze River Metallogenic Belt, Eastern China: Magmatic Response to Early Cretaceous Lithospheric Extension[J]. *Lithos*, 2010, 119: 427-438.
- [79] Liu J, Mao J W, Ye H S, et al. Zircon LA-ICPMS U-Pb Dating of Hukeng Granite in Wugongshan Area, Jiangxi Province and Its Geochemical Characteristics[J]. *Acta Petrologica Sinica*, 2008, 24(8): 1813-1822.
- [80] Wang J Q, Shu L S, Santosh M, et al. The Pre-Mesozoic Crustal Evolution of the Cathaysia Block, South China: Insights from Geological Investigation, Zircon U-Pb Geochronology, Hf Isotope and REE Geochemistry from the Wugongshan Complex[J]. *Gondwana Research*, 2014, 28(1): 225-245.
- [81] Ma T Q, Bai D Y, Kuang J, et al. Zircon SHRIMP Dating of the Xitian Granite Pluton, Chaling, Southeastern Hunan and Its Geological Significance[J]. *Geological Bulletin of China*, 2005, 24: 415-419.
- [82] Fu J M, Ma C Q, Xie C F, et al. The Determination of the Formation Ages of the Xishan Volcanic-Intrusive Complex in Southern Hunan Province[J]. *Acta Geoscientia Sinica*, 2004, 25: 303-308.
- [83] Fu J M, Ma C Q, Xie C F, et al. SHRIMP U-Pb Zircon Dating of the Jiuyishan Composite Granite in Hunan and Its Geological Significance [J]. *Geotectonica et Metallogenia*, 2004, 28(4): 370-378.
- [84] Lu Y F, Ma L Y, Qu W J, et al. U-Pb and Re-Os Isotope Geochronology of Baoshan Cu-Mo Polymetallic Ore Deposit in Hunan Province[J]. *Acta Petrologica Sinica*, 2006, 22(10): 2483-2492.
- [85] 弥佳茹, 袁顺达, 轩一撒, 等. 湖南宝山-大坊矿区成矿花岗岩闪长斑岩的锆石U-Pb年龄、Hf同位素及微量元素组成对区域成矿作用的指示[J]. *岩石学报*, 2018, 34(9): 2548-2564.
- Mi Jiaru, Yuan Shunda, Xuan Yisa, et al. Zircon U-Pb Ages, Hf Isotope and Trace Element Characteristics of the Granodiorite Porphyry from the Baoshan-Dafang Ore District, Hunan: Implications for Regional Metallogeny[J]. *Acta Petrologica Sinica*, 2018, 34(9): 2548-2564.
- [86] Yuan Y B, Yuan S D, Chen C J, et al. Zircon U-Pb Ages and Hf Isotopes of the Granitoids in the Huangshaping Mining Area and Their Geological Significance[J]. *Acta Petrologica Sinica*, 2014, 30(1): 64-78.
- [87] Zhu J C, Huang G F, Zhang P H, et al. On the Emplacement Age and Material Sources for the Granites of Cailing Supersuite, Qitianling Pluton, South Hunan Province[J]. *Geological Review*, 2003, 49: 245-252.
- [88] Xu X S, O'Reilly S Y, Griffin W L, et al. Relict Proterozoic Basement in the Nanling Mountains (SE China) and Its Tectonothermal Overprinting [J]. *Tectonics*, 2005, 24: 1-16.
- [89] Huang H Q, Li X H, Li Z X, et al. Formation of the Jurassic South China Large Granitic Province: Insights from the Genesis of the Jiufeng Pluton[J]. *Chemical Geology*, 2015, 401: 43-58.
- [90] Guo C L, Wang D H, Chen Y C, et al. Precise Zircon SHRIMP U-Pb and Quartz Vein Rb-Sr Dating of Mesozoic Taoxikeng Tungsten Polymetallic Deposit in Southern Jiangxi [J]. *Mineral Deposits*, 2007, 20(4): 432-442.
- [91] Zhang W L, Hua R M, Wang R C, et al. New Dating of the Piaotang Granite and Related Tungsten Mineralization in Southeastern Jiangxi [J]. *Acta Geologica Sinica*, 2009, 83(5): 659-670.
- [92] Liu F Y, Wu J H, Liu S. Early Cretaceous Zircon SHRIMP U-Pb Age of the Trachyte and Its

- Significances of the Gan-Hang Belt [J]. Journal of East China Institute of Technology (Natural Science Edition), 2009, 32(4): 330 - 335.
- [93] Feng C Y, Feng Y D, Xu J X, et al. Isotope Chronological Evidence for Upper Jurassic Petrogenesis and Mineralization of Altered Granite - Type Tungsten Deposits in the Zhangtiantang Area, Southern Jiangxi [J]. Geology in China, 2007, 34 (4): 642 - 650.
- [94] 张文兰, 华仁民, 王汝成, 等. 赣南大吉山花岗岩成岩与钨矿成矿年龄的研究 [J]. 地质学报, 2006, 80(7): 956 - 962.
Zhang Wenlan, Hua Renmin, Wang Rucheng, et al. New Dating of the Dajishan Granite and Related Tungsten Mineralization in Southern Jiangxi [J]. Acta Geologica Sinica, 2006, 80(7): 956 - 962.
- [95] Chen Z G, Li X H, Li W Y, et al. SHRIMP U - Pb Zircon Age of the Quannan Syenite, Southern Jiangxi: Constraints on the Early Yanshanian Tectonic Setting of SE China [J]. Geochimica, 2003, 32(3): 223 - 229.
- [96] Yu J H, Zhou X M, Zhao L, et al. Mantle-Crust Interaction Generating the Wuping Granites: Evidenced from Sr - Nd - Hf - U - Pb Isotopes [J]. Acta Petrologica Sinica, 2008, 21(3): 651 - 664.
- [97] Wang L J, Yu J H, Xu X S, et al. Formation Age and Origin of the Gutian-Xiaotao Granitic Complex in the Southwestern Fujian Province, China [J]. Acta Petrologica Sinica, 2007, 23(6): 1470 - 1484.
- [98] Huang H Q, Li X H, Li W X, et al. Age and Origin of the Dadongshan Granite from the Nanling Range: SHRIMP U - Pb Zircon Age, Geochemistry and Sr - Nd - Hf Isotopes [J]. Geological Journal of China Universities, 2008, 14(3): 317 - 333.
- [99] Xu X S, Deng P, O'Reilly S Y, et al. Single Zircon LA - ICPMS U - Pb Dating of Guidong Complex (SE China) and Its Petrogenetic Significance [J]. Chinese Science Bulletin, 2003, 48(17): 1892 - 1899.
- [100] Zhang W H, Wang C Z, Li X M, et al. A Primary Discussion on Magmatic Evolution Series in the Zijinshan Area, Fujian Province: Evidences from Zircon SIMS U - Pb Ages and Hf, O Isotopes [J]. Bulletin of Mineralogy, Petrology and Geochemistry, 2017, 36(1): 98 - 111.
- [101] Zhao X L, Mao J R, Chen R, et al. Zircon SHRIMP Age and Geochemical Characteristics of the Caixi Pluton in Southwestern Fujian Province [J]. Acta Petrologica et Mineralogica, 2007, 26(3): 223 - 231.
- [102] Li X H, Chung S L, Zhou H W, et al. Jurassic Intraplate Magmatism in Southern Hunan-Eastern Guangxi: $^{40}\text{Ar}/^{39}\text{Ar}$ Dating, Geochemistry, Sr - Nd Isotopes and Implications for the Tectonic Evolution of SE China [J]. Geological Society, London, Special Publications, 2004, 226: 193 - 215.
- [103] Li X H, Li W X, Wang X C, et al. Role of Mantle-Derived Magma in Genesis of Early Yanshanian Granites in the Nanling Range, South China: In Situ Zircon Hf - O Isotopic Constraints [J]. Science in China (Series D), 2009, 52(9): 1262 - 1278.
- [104] 朱金初, 张佩华, 谢才富, 等. 南岭西段花山-姑婆山侵入岩带锆石 U - Pb 年龄格架及其地质意义 [J]. 岩石学报, 2006, 22(9): 2270 - 2278.
Zhu Jinchu, Zhang Peihua, Xie Caifu, et al. Zircon U - Pb Age Framework of Huashan-Guposhan Intrusive Belt, Western Part of Nanling Range, and Its Geological Significance [J]. Acta Petrologica Sinica, 2006, 22(9): 2270 - 2278.
- [105] 蔡永丰, 刘风雷, 冯佐海, 等. 桂东北姑婆山岩体矿物学和年代学特征及其成岩成矿意义 [J]. 吉林大学学报(地球科学版), 2020, 50(3): 842 - 856.
Cai Yongfeng, Liu Fenglei, Feng Zuohai, et al. Mineral Compositional and Chronological Characteristics of Guposhan Pluton in Guangxi and Its Petrogenetic and Metallogenic Significance [J]. Journal of Jilin University (Earth Science Edition), 2020, 50(3): 842 - 856.
- [106] Li Z X, Li X H. Formation of the 1 300 km Wide Intracontinental Orogen and Postorogenic Magmatic Province in Mesozoic South China: A Flat-Slab Subduction Model [J]. Geology, 2007, 35: 179 - 182.
- [107] Xu X S, Lu W M, He Z Y. Age and Generation of Fogang Granite Batholith and Wushi Diorite-Hornblende Gabbro Body [J]. Science in China (Series D), 2007, 37(1): 27 - 38.
- [108] Qiu J S, Hu J, Wang X L, et al. The Baishigang Pluton in Heyuan, Guangdong Province: A Highly Fractionated I - Type Granite [J]. Acta Geologica Sinica, 2005, 79(4): 503 - 514.
- [109] Huang H Q, Li X H, Li Z X, et al. Intraplate Crustal Remelting as the Genesis of Jurassic High - K Granites in the Coastal Region of the Guangdong Province, SE China [J]. Journal of Asian Earth Sciences, 2013, 74: 280 - 302.

- [110] Campbell S, Sewell R, Davis D, et al. New U - Pb Age and Geochemical Constraints on the Stratigraphy and Distribution of the Lantau Volcanic Group, Hong Kong [J]. *Journal of Asian Earth Sciences*, 2007, 31: 139 - 152.
- [111] Su H M, Mao J W, Santosh M, et al. Petrogenesis and Tectonic Significance of Late Jurassic-Early Cretaceous Volcanic-Intrusive Complex in the Tianhuashan Basin, South China [J]. *Ore Geology Reviews*, 2014, 56: 566 - 583.
- [112] Li C L, Wang Z X, Lü Q T, et al. Mesozoic Tectonic Evolution of the Eastern South China Block: A Review on the Synthesis of the Regional Deformation and Magmatism [J]. *Ore Geology Reviews*, 2021, 131: 104028.
- [113] Peng H W, Fan H R, Jiang P, et al. Two-Stage Rollbacks of the Paleo-Pacific Plate Beneath the Cathaysia Block During Cretaceous: Insights from A-Type Granites and Volcanic Rocks [J]. *Gondwana Research*, 2021, 97: 158 - 175.
- [114] Li Z, Qiu J S, Yang X M. A Review of Geochronology and Geochemistry of Late Yanshanian (Cretaceous) Plutons Along the Fujian Coastal Area of Southeastern China: Implications for Magma Evolution Related to Slab Break-off and Rollback in the Cretaceous [J]. *Earth-Science Reviews*, 2014, 128: 232 - 248.
- [115] Liu L, Xu X S, Xia Y. Asynchronizing Paleo-Pacific Slab Rollback Beneath SE China: Insights from the Episodic Late Mesozoic Volcanism [J]. *Gondwana Research*, 2016, 37: 397 - 407.
- [116] Xia Y, Xu X S, Liu L. Transition from Adakitic to Bimodal Magmatism Induced by the Paleo-Pacific Plate Subduction and Slab Rollback Beneath SE China: Evidence from Petrogenesis and Tectonic Setting of the Dike Swarms [J]. *Lithos*, 2016, 244: 182 - 204.
- [117] Zhao L, Guo F, Zhang X B, et al. Cretaceous Crustal Melting Records of Tectonic Transition from Subduction to Slab Rollback of the Paleo-Pacific Plate in SE [J]. *Lithos*, 2021, 384/385: 105982.
- [118] 郭锋,赵亮,张晓兵,等.华南陆块东部晚中生代岩浆作用的深部动力学过程 [J]. *大地构造与成矿学*, 2022, 46(3): 416 - 434.
- Guo Feng, Zhao Liang, Zhang Xiaobing, et al. Geodynamics of Late Mesozoic Magmatism in the Eastern South China Block: An Overview [J]. *Geotectonica et Metallogenia*, 2022, 46(3): 416 - 434.
- [119] Guo F, Wu Y M, Zhang B, et al. Magmatic Responses to Cretaceous Subduction and Tearing of the Paleo-Pacific Plate in SE China: An Overview [J]. *Earth-Science Reviews*, 2021, 212(1): 103448.
- [120] Guo F, Fan W M, Li C W, et al. Multi-Stage Crust-Mantle Interaction in SE China: Temporal, Thermal and Compositional Constraints from the Mesozoic Felsic Volcanic Rocks in Eastern Guangdong-Fujian Provinces [J]. *Lithos*, 2012, 150: 62 - 84.
- [121] Chen Y, Li W, Yuan X, et al. Tearing of the Indian Lithospheric Slab Beneath Southern Tibet Revealed by SKS-Wave Splitting Measurements [J]. *Earth and Planetary Science Letters*, 2015, 413: 13 - 24.
- [122] Li Z L, Zhou J, Mao J R, et al. Zircon U - Pb Geochronology and Geochemistry of Two Episodes of Granitoids from the Northwestern Zhejiang Province, SE China: Implication for Magmatic Evolution and Tectonic Transition [J]. *Lithos*, 2013, 179: 334 - 352.